J. Appl. Comput. Mech., 5(2) (2019) 414-440
DOI: 10.22055/JACM.2018.26398.1330

ISSN: 2383-4536
jacm.scu.ac.ir

M&MoCS
Shahid Chamran University of Ahvaz
Journal of Applied and Computational Mechanics

Research Paper

Isogeometric Topology Optimization of Continuum Structures using an Evolutionary Algorithm

N.S.S. Sahithi, K.N.V. Chandrasekhar

[1] Department of Civil Engineering, CVR College of Engineering, Hyderabad, Telangana 501510, India.

Received June 30 2018; Revised September 24 2018; Accepted for publication October 08 2018.
Corresponding author: K.N.V. Chandrasekhar, Biml.koralla1@gmail.com

Abstract. Topology optimization has been an interesting area of research in recent years. The main focus of this paper is to use an evolutionary swarm intelligence algorithm to perform Isogeometric Topology optimization of continuum structures. A two-dimensional plate is analyzed statically and the nodal displacements are calculated. The nodal displacements using Isogeometric analysis are found to be in good agreement with the nodal displacements acquired by standard finite element analysis. The sizing optimization of the beam is then performed. In order to determine the stress at each point in the beam a formulation is presented. The optimal cross-section dimensions by performing Isogeometric analysis are acquired and verified with the cross-section dimensions achieved by hiring bending stress and shear stress criteria, as well. The topology optimization of a two-dimensional simply supported plate continuum and a problem on three-dimensional continuum are optimized and presented. The results show that the minimum weight which is found by applying Isogeometric topology optimization gives better results compared to the traditional finite element analysis.

Keywords: Swarm Intelligence, Nature Inspired, Isogeometric Analysis, Topology Optimization, NURBS

1. Introduction

The future of Computer Aided Design (CAD) and Finite Element Analysis (FEA) is much closer and the Isogeometric analysis unifies the fields of CAD and FEA. Computational geometry and computational mechanics have become a sophisticated and complex discipline, lately. The Isogeometric analysis adds capabilities to the existing finite element computer programs which include a wide variety of applications. The unique feature of Isogeometric analysis over the traditional finite element analysis is the exact representation of the geometry in the engineering design. Hughes (Hughes et. al., 2005), in his paper, hired Non-Uniform Rational B-Spline (NURBS) basis functions and discussed their unique properties on a wide variety of applications. They also discussed how the research on these powerful functions might benefit several fields. Particular attention is given to the Galerkin finite element method within the framework of Isogeometric analysis.

The isogeometric analysis uses NURBS basis functions which can represent the geometry of the structure more precisely than the finite element methods. The advantage of hiring IGA over traditional finite element analysis is the feature of integrating CAD geometry with the analysis (Hughes et. al., 2005). The required computational effort can be considerably reduced by using fewer numbers of knots to precisely represent the geometry of the structure. The governing differential equations can be solved by Galerkin weak formulation and B-splines or NURBS. The field of Isogeometric analysis is evolving and several problems in engineering field are addressed.

Swarm intelligence is the discipline that deals with natural and artificial systems composed of many individuals that coordinate using decentralized control and self-organization. Swarm Intelligence algorithms are a sub-class of evolutionary algorithms. Firefly algorithm proposed by Yang (Yang, 2009) is one of such nature inspired algorithms which is based on the behavior of fireflies when looking for their food. Fireflies communicate by flashing their light. Dimmer fireflies are attracted to the brighter ones and move towards them to mate. Firefly algorithm is generally employed to solve reliability and redundancy

Published online: April 02 2019

problems (Yang, 2010). The main applications of firefly algorithm are digital image compression and processing, featured selection and fault detection, antenna design, structural design, scheduling, semantic web composition, chemical phase equilibrium, clustering, dynamic problems, and so on. (Archana, 2017).

In this study, Section 1.1 presents the objectives of the study to determine the optimal distribution of material having minimum weight using Isogeometric analysis and evolutionary algorithms. Section 2 discusses the literature review of the work done by several authors who applied Isogeometric analysis in structural mechanics. Section 3 will represent the theory behind the formulation of plate problems. The NURBS basis functions are clearly explained. Section 4 shed lights on the problem statement. In Section 5, a flowchart of the method used to perform topology optimization is presented and discussed. In Section 6, analysis of plate problems in two-dimensions is presented. In section 7, the sizing optimization of a beam is offered. In section 8, the topology optimization of a simply supported two-dimensional plate and a three-dimensional domain are presented. Section 9 briefly concludes the work done in this paper and sets a direction for future studies.

1.1 Objectives of the study

a) Performing the Isogeometric topology optimization of continuum structures using an evolutionary algorithm.

b) Determining the minimum weight distribution of material which is subjected to the constraints of stress and displacement.

1.2 Assumption of the study

a) The material obeys Hooke's law.

b) Buckling analysis is not included in this study.

2. Literature review

The concept of Isogeometric Analysis was first introduced by T.R.J Hughes (Hughes, 2005) and his colleagues at the University of Texas at Austin. The basic idea of IGA is to represent the geometry accurately. The initial work of Isogeometric analysis was first developed to fill the gap between FEA and CAD.

The exact geometric model is generated with basis functions from NURBS (Non-Uniform Rational B-Splines) which is a new method for analysis of solids, fluids, structures and other types of problems which are governed by partial differential equations. This method, not only helps with generating the exact geometric model, but also assists with simplifying mesh refinement by eliminating the need for communication with the CAD geometry after the initial mesh is constructed (Attila, 2010).

Nguyen, *et al.* (Nguyen, 2015) discussed the concepts of Isogeometric analysis in details. A brief introduction to NURBS functions is done. The preliminary concepts and implementation of IGA have been discussed. With the help of Matlab®, the difference between IGA and conventional FEA has been explained with an overview of recent developments and shortcomings of IGA. IGA is mostly helpful for the plate and shell type of problems as NURBS basis functions allows straightforward construction and it is particularly helpful for thin shells as it constructs a rotation free formulation. NURBS also provides advantages for structural vibration problems. IGA is much helpful in solving partial differential equations of fourth-order derivate. This paper also discussed the shortcomings of NURBS. NURBS always produces watertight geometries which always complicates mesh generation. They have also presented Matlab® implementation for one, two, and three-dimensional Isogeometric finite element analysis for structural and solid mechanics.

Luis (Luis, 2011) applied the Isogeometric analysis to perform linear and non-linear analysis of a few basic structural problems in engineering. Mit (Mit, 2015a), in his paper, did a review on the application of Isogeometric analysis for problems in one-dimensional, two-dimensional, and three-dimensional cases. Gondegaon (Gondegaon, 2016) performed the static and modal analysis of few basic problems. Gondegaon (Gondegaon, 2014) applied IGA to model the geometry which exactly represents the domain. Nguyen (Nguyen, 2015) has presented the computer implementation aspects for several problems in engineering. Hartman (Hartman, 2011) applied Isogeometric analysis to LS-Dyna and concludes that the IGA gives better results over traditional methods with less computational effort. Mit (Mit, 2015b) in another paper, performed stress calculations using Isogeometric analysis. Nagy (Nagy, 2010) used variational formulation and applied Isogeometric analysis to solve the differential equations by Galerkin weak formulation. Mateus (Mateus, 2013) employed Isogeometric analysis to perform free vibrational analysis of bars. Laura (Laura, 2012) presented a few open issues in Civil Engineering which include interface modeling. Milos (Milos, 2016) discussed the free vibration analysis of beam structures using Isogeometric concept. Clough and Penzien (Clough, 1993) argued the formulation of stiffness matrix and mass matrix for beams and bars.

In Civil engineering, beam elements are primary components in a structure. A free vibration analysis is required for a beam as it is always subjected to some dynamic excitation. The traditional method hired for this type of excitation is the Bernoulli-Euler beam. For thick beams, transverse shear deformation and rotatory inertia effect are included in Timoshenko beam as they give more adequate results. Milos (Milos, 2016) has used Isogeometric analysis approach for free vibration analysis beam and compared it with dynamic stiffness method (DSM) and conventional finite element method (FEM). Valizadeh (Valizadeh, 2011) employed an improved Isogeometric analysis by employing the Lagrange Multiplier method. For the purpose of designing the structural systems, earlier they used to plan a general layout which efficiently supports the predicted design loads. This prediction of the structural design systems is generally done by either fixed or variable topology shape optimization. There are two techniques which are helpful for optimizing the shape and topology of the system. Ohsaki (Ohsaki and Swan, 2002) mainly focused on the topology optimization of trusses and frames with a detailed explanation of the two techniques with some example problems on continuum optimization.

Firefly algorithm is proposed by XS Yang in 2008 which is based on the flashing rhythmic pattern of the flies to find their potential prey. The role of evolutionary algorithms to perform the optimization is evident from the researches over the number of years. A taxonomy of the algorithms is presented by Weiss (2009) as shown in Fig.1. The included dotted-line shows that the firefly algorithm can be classified under the heading of swarm intelligence algorithms. A brief list of contributors to the optimization algorithms which included here is given in Table 1 for the sake of convenience and ease. The list starts with Genetic algorithms by John Holland in 1975 to date.

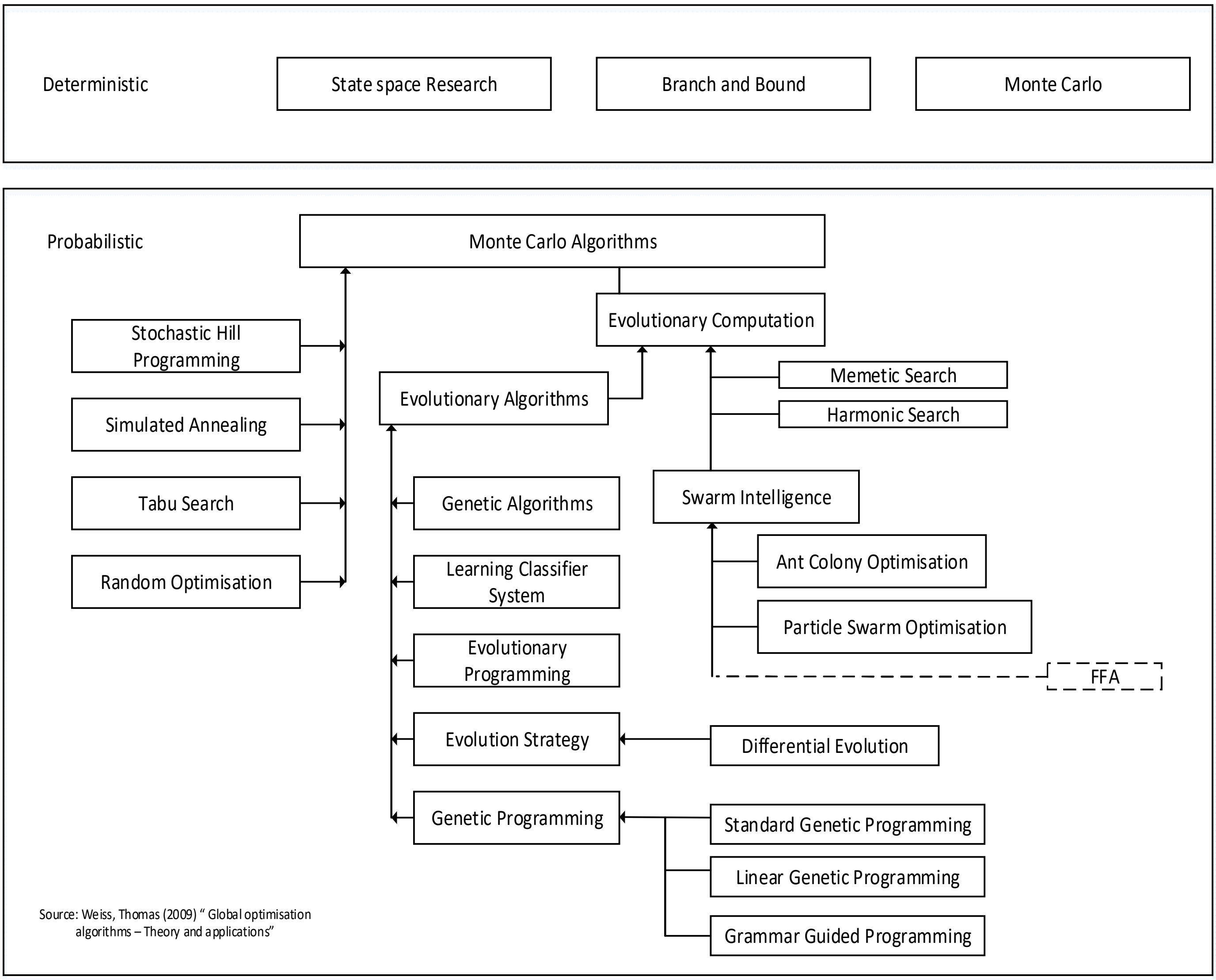

Fig. 1. Taxonomy of the global optimization algorithms (Weiss, 2009). Note that the dotted-line is not in the original flowchart. The dotted-line is added later to identify the FFA in the classification chart.

The field of structural optimization rejuvenated with the advent of computers during the mid-1960's and then on. The list of contributors in the field of optimization starting with John Holland in 1975 is given here in Table 1. The presented list of contributions is not complete and there might be several researches who may not be on the list.

2.1 Connectivity Analysis (Hsu and Hsu, 2005a)

Connectivity analysis will identify all the elements above the threshold value and also has an edge/face connectivity with other elements connecting all seed elements within the given continuum. In other words, all the elements having an edge or a corner connectivity and/or not connected will be assigned a very small density value equal to 1e-5 during the analysis. Figure 2(a) shows an example of elements that are not connected and figure 2(b) displays two elements which are connected with a face connectivity in common.

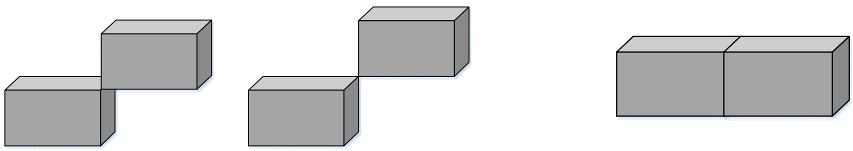

(a) (b)

Fig. 2. The connectivity criteria (a) Not connected elements (b) Connected elements - Face connectivity

FE analysis is performed by using a constant meshing technique in which all the elements in the structure will be considered during the analysis and all the elements without connectivity are assigned a lower density value of 1e-5. (Hsu, 2005b)

Table 1. The list of contributors to the field of optimization (Archana, 2017)

Number	Year	Algorithms since 1975
1	1975	Holland proposed Genetic Algorithms (GA)
2	1977	Glover proposed Scatter Search (SS)
3	1980	Smith genetic programming (GP)
4	1983	Kirk Patrick's Simulated Annealing (SA)
5	1986	Glover and McMillan offered Tabu Search (TS)
6	1986	Farmer et al. suggested the Artificial immune system (AIS)
7	1988	Koza registered first patent on Genetic programming
8	1989	Evolver provided the first optimization software using GA
9	1989	Moscate presented Memetic Algorithm (MA)
10	1992	Dorigo proposed Ant Colony Optimization (ACO)
11	1993	Fonseca and Flemming provided multi objective GA
12	1994	Battiti and Tecchiolli introduced Reactive Search optimization
13	1995	Kennedy and Eberhardt proposed PSO
14	1997	Storn and Price proposed differential evolution
15	1997	Rubenstien presented Cross Entropy method
16	1999	Tillard and Voss proposed POPMUSIC
17	2000	Snyman Leap Frog algorithm
18	2001	Geem provided Harmony Search
19	2001	Hansetha nd Aanestad offered Bootstrap Algorithm
20	2004	Nakrani and Tovey presented Bees Optimization
21	2005	Krishnanand and Ghose introduce Glow Worm optimization
22	2005	Karaboga proposed Artificial Bee Colony algorithm
23	2006	Haddad et al. proposed Honey Bee Mating optimization
24	2007	Hamed Shah Hosseini offered Intelligent Water Drops
25	2007	Atashpaz et al. introduced Imperialist Competitive algorithm
26	2008	Yang presented Firefly algorithm
27	2008	Mucherino Seref suggested Monkey search
28	2009	Husseinzadeh provided League Championship algorithm
29	2009	Rashedi et al. introduced Gravitational Search algorithm
30	2009	Yang and Deb offered Cuckoo search
31	2010	Yang developed Bat algorithm
32	2010	Kaveh proposed Charged search system
33	2011	Shah Hosseini introduced Galaxy based search
34	2011	Tamura and Yasuda designed Spiral optimization
35	2011	Rao et al. presented Teaching Learning based optimization
36	2012	Gandomi proposed Krill Herd algorithm
37	2012	Civicioglu introduced Differential Search algorithm
38	2014	Kaveh Magnetic Search system
39	2016	Kaveh proposed Evaporation algorithm
40	2016	Chandrasekhar proposed Aqua Search algorithm to cater large search domains for continuum structures

2.2 Seed element

Elements with supports or carrying the load will have material at all times during the optimization. The density of the elements is equal to one. (Hsu et.al., 2009)

2.3 Stress-based proportioning (Reddy, 2017)

The distribution of material is done based on the stress carried by the element. In other words, the element carrying more stress will be having a higher density value and the element having lower stress will have a lower density value. The density is computed as follows:

$$Relative\ Density = \frac{maximum\ principal\ stress\ carried\ by\ the\ element}{maximum\ principal\ stress\ carried\ by\ the\ structure}$$

The density value varies in the interval of [0, 1]. This should ensure that the material distribution is done efficiently by identifying the elements which can carry material. Furthermore, the newer configuration of material distribution in the structure can be effectively used to safely transmit the loads.

2.4 A Move is counted when one particle, I, moves towards the particle, J, with lower weight. One move requires two FE computations. One iteration is complete when all the individuals move towards the other individuals with lower weight. One run has several iterations.

3. Theoretical Background

The theory behind the knot vectors for a quadratic and a cubic curve are discussed here.

Quadratic

When the degree of the curve is p=2, the support is over p+1 knot spans. The knot vector of p+1+1 knots is required to calculate the basis functions.
The element is defined using a knot span and the basis functions are valid for the knot span. The knot span is different for each element and the corresponding basis functions have to be calculated separately for each element.
For example, p=2 and knot vector is {0, 0, 0, 1/4, 2/4, 3/4, 4/4, 4/4, 4/4}. The number of local knots per element is equal to four, which means that the basis functions are (N_1 N_2 N_3).

Table 2. Local knot vector and Greville points for quadratic curve

Local knot vector	Greville Points for Identifying parameterization only
0 0 0 1/4	0.5 * (0+0) = 0
0 0 1/4 2/4	0.5 * (0+1/4) = 1/8
0 1/4 2/4 3/4	0.5 * (1/4+1/2) = 3/8
1/4 2/4 3/4 1	0.5 * (1/2+3/4) = 5/8
2/4 3/4 1 1	0.5 * (3/4+1) = 7/8
3/4 1 1 1	0.5 * (1+1) = 1

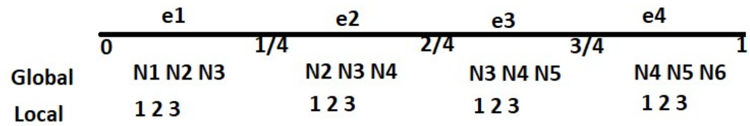

The IGA elements are rotation free elements. The continuity can be maintained by having knots in common. For a quadratic degree, there are two knots in common and for a cubic degree curve there are three knots in common.

Cubic curve

When the degree of the curve is p=3, the support is over p+1 knot spans. The knot vector of p+1+1 knots is required to calculate the basis functions.
The element is defined using a knot span and the basis functions are valid for a knot span. The knot span is different for each element and the corresponding basis functions have to be calculated separately for each element.
For example, p=3 and knot vector is {0, 0, 0, 0, 1/4, 2/4, 3/4, 4/4, 4/4, 4/4, 4/4}. The number of knots is equal to five per element, which means that the basis functions are (N_1 N_2 N_3 N_4).

Table 3. Local knot vector and Greville points for cubic curve

Local knot vector	Greville Points for Identifying parameterization only
0 0 0 0 1/4	(1/3) * (0+0+0) = 0
0 0 0 1/4 2/4	(1/3) * (0+0+1/4) = 1/12
0 0 1/4 2/4 3/4	(1/3) * (0+1/4+1/2) = 1/4 = 3/12
0 1/4 2/4 3/4 1	(1/3) * (1/4+1/2+3/4) = 1/2 = 6/12
1/4 2/4 3/4 1 1	(1/3) * (2/4+3/4+1) = 3/4 = 9/12
2/4 3/4 1 1 1	(1/3) * (3/4+1+1) = 11/12
3/4 1 1 1 1	(1/3) * (1+1+1) = 12/12

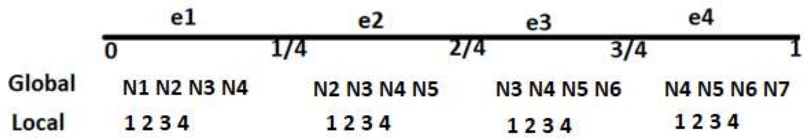

The IGA elements are rotation free elements. The continuity can be maintained by having knots in common. For a quadratic degree, there are two knots in common and for a cubic degree curve three knots are in common.
The problems in structural mechanics require control points to be defined at the points where deflection has to be calculated. The control points can be defined at equal intervals over the entire length of the beam. The behavior can be non-linear in such cases.

3.1 NURBS Formulation

The basic theory is presented in this section. The NURBS basis functions and the parent to parametric mapping are discussed. The strain-displacement matrix is presented and then forms the stiffness matrix. In Section 6, an example of a two-dimensional plate continuum is analyzed using Isogeometric analysis. The NURBS basis functions are employed and are discussed first. The stiffness matrix is derived in a step-wise manner. The solution for the displacement vector at each node is compared with the results from the standard finite element analysis. The achieved results show that the nodal displacements using Isogeometric analysis are in good agreement with the results found by using standard finite element analysis.

3.1.1 Basis Functions

The basis functions are given by

$$N_{i,0}(\xi) = \begin{Bmatrix} 1 & if\ \xi_i \le \xi < \xi_{i+1} \\ 0 & otherwise \end{Bmatrix} \tag{1}$$

For p = 1, 2, 3, …. They are defined by

$$N_{i,p}(\xi) = \frac{\xi - \xi_i}{\xi_{i+p} - \xi_i} N_{i,p-1}(\xi) + \frac{\xi_{i+p+1} - \xi}{\xi_{i+p+1} - \xi_{i+1}} N_{i+1,p-1}(\xi) \tag{2}$$

This is referred to as the Cox-de Boor recursion formula.

3.1.2 Derivatives of B-Spline Basis functions

The derivatives of the basis functions are given by

$$\frac{d}{dx} N_{i,p}(\xi) = \frac{p}{\xi_{i+p} - \xi_i} N_{i,p-1}(\xi) - \frac{p}{\xi_{i+p+1} - \xi_{i+1}} N_{i+1,p-1}(\xi) \tag{3}$$

3.1.3 Generalize to higher order derivatives

The generalized higher order derivatives of the basis functions are given as

$$\frac{d^k}{d^k\xi} N_{i,p}(\xi) = \frac{p}{\xi_{i+p} - \xi_i} \left(\frac{d^{k-1}}{d^{k-1}\xi} N_{i,p-1}(\xi) \right) - \frac{p}{\xi_{i+p+1} - \xi_{i+1}} \left(\frac{d^{k-1}}{d^{k-1}\xi} N_{i+1,p-1}(\xi) \right) \tag{4}$$

3.1.4 B-spline curves

The B-spline curve is given by

$$C(\xi) = \sum_{i=1}^{n} N_{i,p}(\xi) B_i \tag{5}$$

3.1.4.1 B-spline surfaces

B-spline surfaces are given by

$$S(\xi,\eta) = \sum_{i=1}^{n} \sum_{j=1}^{m} N_{i,p}(\xi) M_{j,q}(\eta)\, B_{i,j} \tag{6}$$

3.1.4.2 B-spline solids

B-spline solids are given as

$$S(\xi,\eta,\zeta) = \sum_{i=1}^{n} \sum_{j=1}^{m} \sum_{k=1}^{l} N_{i,p}(\xi) M_{j,q}(\eta) L_{k,r}(\zeta)\, B_{i,j,k} \tag{7}$$

3.1.5 NURBS Basis Function

With a given projective B-spline curve and its associated projective control points in hand, the control points for the NURBS curve are acquired by the following relations:

$$(B_i)_j = \frac{(B_i^w)_j}{w_i}\; j = 1,2 \dots, d \tag{8}$$

NURBS basis is given by $w_i = (B_i^w)_{jd+1}$.

3.1.5.1 For NURBS curve

The NURBS curve is given by

$$R_i^p(\xi) = \frac{N_{i,p}(\xi) w_i}{\sum_{i=1}^{n} N_{i,p}(\xi) w_i}$$
$$C(\xi) = \sum_{i=1}^{n} R_i^p(\xi) B_i \tag{9}$$

This is identical to the B-Splines.

3.1.5.2 For NURBS surfaces

The NURBS surfaces are given by

$$R_{i,j}^{p,q}(\xi,\eta) = \frac{N_{i,p}(\xi) M_{j,q}(\eta) w_{i,j}}{\sum_{i=1}^{n} \sum_{j=1}^{m} N_{i,p}(\xi) M_{j,q}(\eta) w_{i,j}} \tag{10}$$

3.1.5.3 For NURBS solids

The NURBS solids are given by

$$R_{i,j,k}^{p,q,r}(\xi,\eta,\zeta) = \frac{N_{i,p}(\xi)M_{j,q}(\eta)L_{k,r}(\zeta)w_{i,j,k}}{\sum_{i=1}^{n}\sum_{j=1}^{m}\sum_{k=1}^{l}N_{i,p}(\xi)M_{j,q}(\eta)L_{k,r}(\zeta)w_{i,j,k}} \tag{11}$$

3.1.5.4 Derivatives of NURBS

Applying the quotient rule, the derivatives of NURBS are given by

$$\frac{d}{d\xi}R_i^p(\xi) = w_i\frac{W(\xi)N_{i,p}^{'}(\xi) - W^{'}(\xi)N_{i,p}(\xi)}{(W(\xi))^2} \tag{12}$$

where

$$N_{i,p}^{'}(\xi) = \frac{d}{d\xi}N_{i,p}(\xi) \; and \; W^{'}(\xi) = \sum_{i=1}^{n}N_{i,p}^{'}(\xi)w_i \tag{13}$$

3.1.5.5 For higher order derivatives of NURBS basis functions

The higher order derivatives of NURBS basis functions are given by

$$A_i^{(k)}(\xi) = w_i\frac{d^k}{d\xi^k}N_{i,p}(\xi)\,, (no\ sum\ on\ i) \tag{14}$$

Do not sum on the repeated index, and let $W^{(k)}(\xi) = \frac{d^k}{d\xi^k}W(\xi)$. Higher order derivatives can be expressed in terms of the lower order derivatives as

$$\frac{d^k}{d\xi^k}R_i^p(\xi) = \frac{A_i^{(k)}(\xi) - \sum_{j=1}^{k}\binom{k}{j}W^{(j)}(\xi)\frac{d^{(k-j)}}{d\xi^{(k-j)}}R_i^p(\xi)}{W(\xi)} \tag{15}$$

where $\binom{k}{j} = \frac{k!}{j!(k-j)!}$.

3.1.6 Parametric to parent mapping

The parametric to parent mapping is given by

$$\xi = \frac{1}{2}[(\xi_{i+1} - \xi_i)\hat{\xi} + (\xi_{i+1} - \xi_i)],\;\; \eta = \frac{1}{2}[(\eta_{i+1} - \eta_i)\hat{\eta} + (\eta_{i+1} - \eta_i)] \tag{16}$$

The Jacobian is given by

$$J_{\bar{\xi},\bar{\eta}} = \frac{1}{4}(\xi_{i+1} - \xi_i)(\eta_{i+1} - \eta_i) \tag{17}$$

3.1.6.1 Parametric space to Physical space

The parametric space to physical space is given by

$$\begin{gathered} X = N_1M_1X_1 + N_2M_1X_2 + N_2M_2X_3 + N_1M_2X_4 \\ Y = N_1M_1Y_1 + N_2M_1Y_2 + N_2M_2Y_3 + N_1M_2Y_4 \end{gathered} \tag{18-a}$$

$$\begin{bmatrix} \frac{\partial N}{\partial \xi} \\ \frac{\partial N}{\partial \eta} \end{bmatrix} = \begin{bmatrix} \frac{\partial x}{\partial \xi} & \frac{\partial y}{\partial \xi} \\ \frac{\partial x}{\partial \eta} & \frac{\partial y}{\partial \eta} \end{bmatrix} \begin{bmatrix} \frac{\partial N}{\partial x} \\ \frac{\partial N}{\partial y} \end{bmatrix} \tag{18-b}$$

where,

$$\begin{aligned} \frac{\partial x}{\partial \xi} &= \frac{\partial}{\partial \xi}\,[N_1M_1\;N_2M_1\;N_2M_2\;N_1M_2][x_1\;x_2\;x_3\;x_4]^T \\ \frac{\partial x}{\partial \eta} &= \frac{\partial}{\partial \eta}\,[N_1M_1\;N_2M_1\;N_2M_2\;N_1M_2][x_1\;x_2\;x_3\;x_4]^T \\ \frac{\partial y}{\partial \xi} &= \frac{\partial}{\partial \xi}\,[N_1M_1\;N_2M_1\;N_2M_2\;N_1M_2][y_1\;y_2\;y_3\;y_4]^T \\ \frac{\partial y}{\partial \eta} &= \frac{\partial}{\partial \eta}\,[N_1M_1\;N_2M_1\;N_2M_2\;N_1M_2][y_1\;y_2\;y_3\;y_4]^T \end{aligned} \tag{18-c}$$

3.1.7 Strain Displacement Matrix

The strain displacement matrix is given by

$$B = \begin{bmatrix} \frac{\partial N}{\partial x} & 0 \\ 0 & \frac{\partial N}{\partial y} \\ \frac{\partial N}{\partial y} & \frac{\partial N}{\partial x} \end{bmatrix} \tag{19-a}$$

The strain vector is given as

$$\epsilon = \begin{bmatrix} \frac{\partial u}{\partial x} \\ \frac{\partial v}{\partial y} \\ \frac{\partial u}{\partial y} + \frac{\partial v}{\partial x} \end{bmatrix} \tag{19-b}$$

where

$$\begin{bmatrix} \frac{\partial u}{\partial x} \\ \frac{\partial u}{\partial y} \end{bmatrix} = \frac{1}{|J|} \begin{bmatrix} J_{22} & -J_{12} \\ -J_{21} & J_{11} \end{bmatrix} \begin{bmatrix} \frac{\partial u}{\partial \xi} \\ \frac{\partial u}{\partial \eta} \end{bmatrix}. \tag{20-a}$$

The strain is given as

$$\epsilon = AG = \frac{1}{|J|} \begin{bmatrix} J_{22} & -J_{12} & 0 & 0 \\ 0 & 0 & -J_{21} & J_{11} \\ -J_{21} & J_{11} & J_{22} & -J_{12} \end{bmatrix} \begin{bmatrix} \frac{\partial u}{\partial \xi} \\ \frac{\partial u}{\partial \eta} \\ \frac{\partial v}{\partial \xi} \\ \frac{\partial v}{\partial \eta} \end{bmatrix}. \tag{20-b}$$

3.1.7.4 Stiffness Matrix

The stiffness matrix is given as

$$k = t \int_{-1}^{1} \int_{-1}^{1} B^T D B \; |J_{\xi,\eta}| \, d\xi \, d\eta \, |J_{\bar{\xi},\bar{\eta}}| \, weight. \tag{21}$$

3.1.7.5 Gauss Quadrature

Assuming the degree of the curve to be p, the thumb rule of p+1 Gauss quadrature is followed. The Gauss quadrature points for 2x2 are given by $\xi = \pm \frac{1}{\sqrt{3}} \eta = \pm \frac{1}{\sqrt{3}}$..

3.1.8 Algorithm to perform the IGA analysis

The algorithm to perform the Isogeometric analysis of a two-dimensional plate structure carrying in-plane loading will be noted subsequently.

1. Determining NURBS coordinates $(\xi_i, \xi_{i+}) * (\eta_j, \eta_{j+1})$
2. Storing the connectivity of the element in an array names B (of size nn)
3. Defining the strain-displacement matrix B of size (1, 2*nn)
4. Setting $k_e = 0$
5. Loop over Gauss points (GPs) $\{\xi_j^{'}, \omega_j^{'}\}$ j= 1,2,…,n_{gp} where ngp is the number of gauss points
   a) Computing parametric coordinate ξ corresponding to $\xi_j^{'}$
   b) Computing $|J_{\xi'}|$ corresponding to the equations
   c) Computing the derivatives of the shape functions $R_{w\xi}^e$ and $R_{w\eta}^e$ at point ξ, η
   d) Computing J_ξ using control points (sctr(:,e)) $R_{w\xi}^e$ and $R_{w\eta}^e$
   e) Finding J_ξ^{-1} and determinant $|J_\xi|$
   f) Computing the shape function derivatives $R_x = J_\xi^{-1}[R_{,\xi}^T R_{,\eta}^T]$
   g) Using R_x to build the strain displacement matrix B

h) $k_e = k_e + B^T DB|J_{\xi'}||J_{\eta'}|\omega_j'$
6. End of the loop on Gauss points
7. Assembling k_e into global stiffness matrix K^G
8. End of the loop over all the elements

3.2 Introduction to the firefly algorithm

Swarm intelligence algorithms which are inspired by nature are becoming more popular in solving optimization problems. One of the most recent examples is the firefly algorithm which combines levy flights to depict the typical flight characteristics of animals and insects. This algorithm was found to be more promising and superior than many other such algorithms. These search strategies performed by using multi-agents are efficient in local search and finding global best solutions (Yang, 2009). The flashing light can be formulated in such a way which is associated with the objective function to be optimized, which makes it possible to formulate new optimization algorithms.

3.2.1 Assumptions

There are three idealized rules which are the key to this algorithm (Yang, 2010).
1. All fireflies are uni-sex, which means that each fly can get attracted to the other one.
2. Attractiveness is proportional to their brightness, for any two flashing flies. The less bright fly moves toward the brighter fly. The attractiveness is proportional to the brightness and they both decrease as their distance increases. If there is no brighter fly, then it will move randomly.
3. The brightness of the fly is determined by the landscape of the objective function. For a maximization problem, the brightness can simply be proportional to the objective function.

3.2.2 Theory

There are two important issues that have to be dealt with which are the variation of light intensity and formulation of attractiveness. The brightness/attractiveness is seen in the eyes of the beholder or judged by other flies. It will vary with the distance, r_{ij}, between firefly i and firefly j. The light intensity decreases with the distance from its source, and light is also absorbed in the media with the attractiveness varying with the degree of absorption. The Cartesian distance between the two fireflies i and j at x_j and x_i is given by (Yang, 2009).

$$r_{ij} = \sqrt{\sum_{k=1}^{d} (x_{i,k} - x_{j,k})^2} \tag{22}$$

where, $x_{i,k}$ is the k^{th} component of the spatial co-ordinate x_i of i^{th} firefly. The movement of the firefly i which is attracted to another attractive (brighter) firefly j is determined by

$$x_i = x_i + \beta_0 e^{-\Upsilon r_{ij}^2}(x_j - x_i) + \alpha \, sign\left[rand - \frac{1}{2}\right] \oplus Levy \tag{23}$$

where the second term is due to the attraction and the third term is randomization via levy flights with α being the randomization parameter. The $sign\left[rand - \frac{1}{2}\right]$ where $rand \in [0,1]$ essentially provide a random sign or direction while the random step length is drawn from a levy distribution whose mean is infinite and variance is infinite. (Yang, 2014)

$$Levy \sim u = t^{-\lambda}, (1 < \lambda \leq 3) \tag{24}$$

$$Levy\ distribution\ is = \frac{1}{\sqrt{2\Pi}} \frac{e^{\frac{-u}{2}}}{u^{3/2}} \tag{25}$$

The steps of firefly are drawn from a levy distribution random walk with a power-law step length distribution with a heavy tail.

3.3 Solid Isotropic Material with Penalization (Bendsoe, 1999)

Martin Phillip Bendsoe and Ole Sigmund (2009) proposed SIMP law to eliminate the elements having intermediate densities during the optimization. The final result can be in a clear black and white output. The Young's modulus of elasticity (E) of these elements has to be penalized using the SIMP law as follows to determine the newer value of Young's modulus of elasticity for each element.

$$E_{new} = \rho^p E_{old} \tag{26}$$

where $'\rho'$ (pronounced as rho) is the relative density and 'p' is the penalization parameter.

4. Problem Statement

The objective is to find the minimum weight (f) of the structure subjected to the constraint on the amount of material used and the stresses in the structure.

$$f = \left(\sum_{i=1}^{n} \rho_i v_i\right) * \bar{\rho} \tag{27}$$

Where ρ_i is the density parameter of the element and v_i is the volume of the element, and $\bar{\rho}$ is the density of the material subjected to $M * v - \left(\sum_{i=1}^{n} \rho_i v_i\right) \geq 0$. (28)

M is the allowable material in percentage, and v is the volume of the structure subjected to Principal stress (29)

$$\sigma_i \leq \sigma_{allow} \quad i = 1,2,3 \tag{30}$$

5. Optimization Process

The flowchart to conduct the Isogeometric topology optimization is as shown in Fig.3.

5.1 Process

The optimization method proposed by Archana (Archana, 2017) is as shown in the Fig.3 to perform the Isogeometric topology optimization of continuum structures. The knot vector is formed first knowing the degree of the curve along each dimension X, Y, and Z. The NURBS basis functions are then derived to form the stiffness matrix for each element and assembled to form the global stiffness matrix for the entire structure. The relative densities for each element are generated initially with values varying from 0 to 1. The initial value of the objective function is calculated. The objective function of each search fly (Firefly algorithm) is then compared with the objective function of the other individuals in the population. The newer values of the relative densities are computed using firefly algorithm and the analysis is then performed. The distribution of material should not only satisfy the connectivity analysis which include the elements carrying forces and the supports but also satisfy the stress criterion, minimum volume criterion as well. After which, the search fly is considered to have a valid distribution of material. This process is repeated until convergence and the search fly with the minimum value of the objective function should have the valid distribution.

5.2 The Program

A Finite element program developed in C++ is used to perform topology optimization on a notebook computer (Intel I7 processor, 4 core, 3.5 GHz with 4GB RAM).

6. Step by Step Analysis of a Two-Dimensional Plates Structures using Isogeometric Analysis

In this section, a two-dimensional cantilever plate structure is analyzed and nodal displacements are determined.

6.1 A square plate carrying in-plane loading

The domain is a cantilever plate 50 mm×50 mm and fixed along the left edge as shown in Fig.4a. The plate is discretized into 25 elements using 36 nodes. The Young's modulus of the material is taken equal to 200 GPa, and the Poisson's ratio is equal to 0.3. The thickness of the plate is unity. The plate is analyzed in-plane stress condition using first-order NURBS curve along both the X and Y directions. The total number of control points is equal to 6×6 = 36. The plate carries a horizontal load of 1257 N each at control points 31 and 36. The plate carries a horizontal load of 2514 N each at the control points 32-35 as shown in Fig.4b. The degree of the NURBS curve is taken as equal to unity along both X and Y directions. The Knot vector Xi along the X-axis is [0 0 0 0.2 0.4 0.6 0.8 1 1 1] as shown in the Fig.4b. The span of knot vector Xi is equal to 10. The knot Vector Eta along the Y-axis is the same as the knot vector Xi. The element node connectivity is as shown in Table 4. The knots for each element are tabulated here. The knots for each element along the X and Y direction are as shown in Table 5. The control points and knots for the plate structure are as shown in Table 6. For each control point, the knot value is given.

Table 4. The element node connectivity

Element e	Node1	Node2	Node3	Node4	Element e	Node1	Node2	Node3	Node4
1	1	2	3	4	13	15	21	22	16
2	2	13	14	3	14	21	27	28	22
3	13	19	20	14	15	27	33	34	28
4	19	25	26	20	16	8	7	9	10
5	25	31	32	26	17	7	16	17	9
6	4	3	5	6	18	16	22	23	17
7	3	14	15	5	19	22	28	29	23
8	14	20	21	15	20	28	34	35	29
9	20	26	27	21	21	10	9	11	12
10	26	32	33	27	22	9	17	18	11
11	6	5	7	8	23	17	23	24	18
12	5	15	16	7	24	23	29	30	24
25	29	35	36	30					

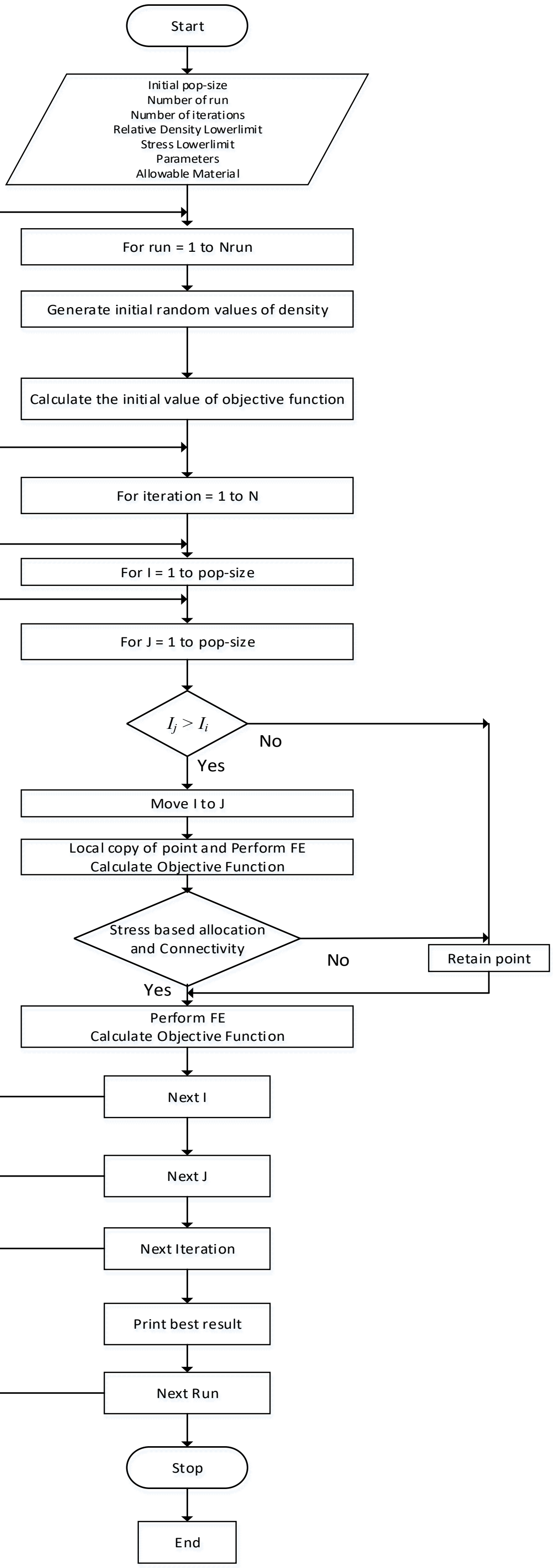

Fig. 3. The flowchart to perform the Isogeometric Topology Optimization

6.1.1 Basis Functions

Important properties of the basis functions as follows

$$N_{i,p}(\xi) = \frac{\xi \; - \xi_i}{\xi_{i+p} - \xi_i} N_{i,p-1}(\xi) + \frac{\xi_{i+p+1} - \xi}{\xi_{i+p+1} - \xi_{i+1}} N_{i+1,p-1}(\xi)$$
$$N_{i,0}(\xi) = \begin{cases} 1 \;\; if \; \xi_i \le \; \xi < \xi_{i+1} \\ 0 \quad otherwise \end{cases} \tag{31}$$

1. They constitute a partition of unity $\sum_{i=1}^{n} N_{i,p}(\xi) = 1$
2. The support for basis function is compact within the interval of $[\xi_i, \xi_{i+p+1}]$
3. The basis functions are positive $\forall\ \xi_i$

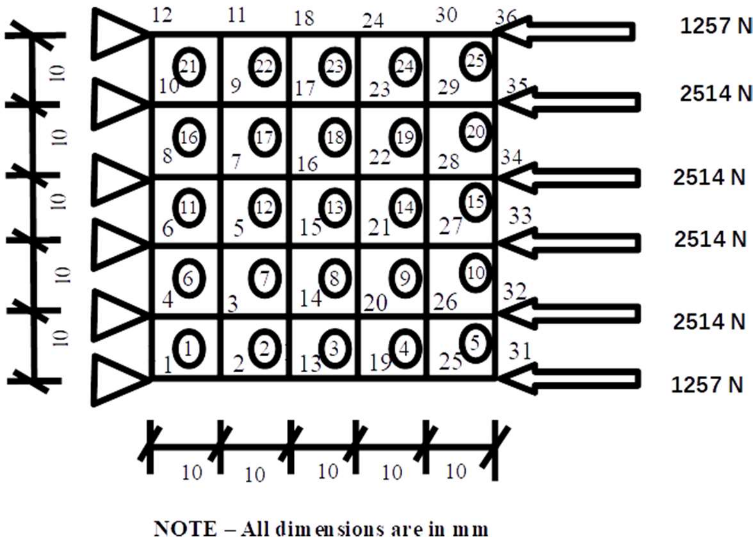

(a)

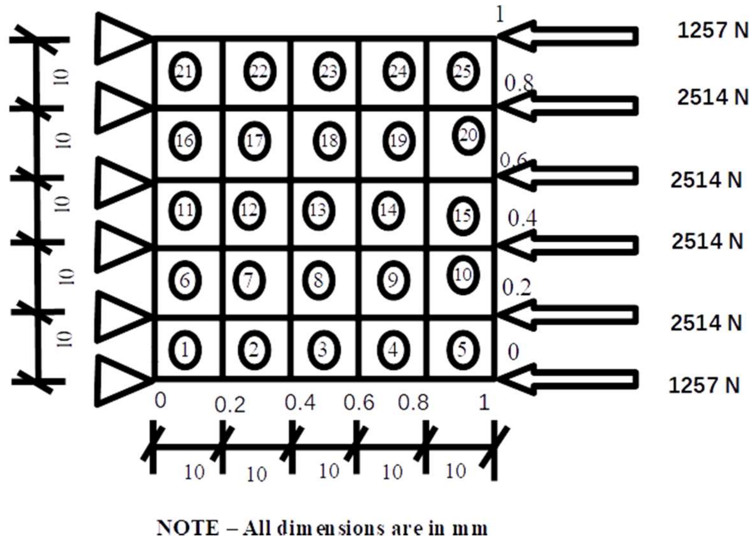

(b)

Fig. 4. (a) The control points at the corners and the element numbers are encircled (b) The knots and the element numbers encircled

Table 5. The Knots for each element along each dimension

Element 1 $\xi = 0$ *and* $\xi = 0.2$ $\eta = 0$ *and* $\eta = 0.2$	Element 2 $\xi = 0.2$ *and* $\xi = 0.4$ $\eta = 0$ *and* $\eta = 0.2$	Element 3 $\xi = 0.4$ *and* $\xi = 0.6$ $\eta = 0$ *and* $\eta = 0.2$	Element 4 $\xi = 0.6$ *and* $\xi = 0.8$ $\eta = 0$ *and* $\eta = 0.2$	Element 5 $\xi = 0.8$ *and* $\xi = 1$ $\eta = 0$ *and* $\eta = 0.2$
Element 6 $\xi = 0$ *and* $\xi = 0.2$ $\eta = 0.2$ *and* $\eta = 0.4$	Element 7 $\xi = 0.2$ *and* $\xi = 0.4$ $\eta = 0.2$ *and* $\eta = 0.4$	Element 8 $\xi = 0.4$ *and* $\xi = 0.6$ $\eta = 0.2$ *and* $\eta = 0.4$	Element 9 $\xi = 0.6$ *and* $\xi = 0.8$ $\eta = 0.2$ *and* $\eta = 0.4$	Element 10 $\xi = 0.8$ *and* $\xi = 1$ $\eta = 0.2$ *and* $\eta = 0.4$
Element 11 $\xi = 0$ *and* $\xi = 0.2$ $\eta = 0.4$ *and* $\eta = 0.6$	Element 12 $\xi = 0.2$ *and* $\xi = 0.4$ $\eta = 0.4$ *and* $\eta = 0.6$	Element 13 $\xi = 0.4$ *and* $\xi = 0.6$ $\eta = 0.4$ *and* $\eta = 0.6$	Element 14 $\xi = 0.6$ *and* $\xi = 0.8$ $\eta = 0.4$ *and* $\eta = 0.6$	Element 15 $\xi = 0.8$ *and* $\xi = 1$ $\eta = 0.4$ *and* $\eta = 0.6$
Element 16 $\xi = 0$ *and* $\xi = 0.2$ $\eta = 0.6$ *and* $\eta = 0.8$	Element 17 $\xi = 0.2$ *and* $\xi = 0.4$ $\eta = 0.6$ *and* $\eta = 0.8$	Element 18 $\xi = 0.4$ *and* $\xi = 0.6$ $\eta = 0.6$ *and* $\eta = 0.8$	Element 19 $\xi = 0.6$ *and* $\xi = 0.8$ $\eta = 0.6$ *and* $\eta = 0.8$	Element 20 $\xi = 0.8$ *and* $\xi = 1$ $\eta = 0.6$ *and* $\eta = 0.8$
Element 21 $\xi = 0$ *and* $\xi = 0.2$ $\eta = 0.8$ *and* $\eta = 1$	Element 22 $\xi = 0.2$ *and* $\xi = 0.4$ $\eta = 0.8$ *and* $\eta = 1$	Element 23 $\xi = 0.4$ *and* $\xi = 0.6$ $\eta = 0.8$ *and* $\eta = 1$	Element 24 $\xi = 0.6$ *and* $\xi = 0.8$ $\eta = 0.8$ *and* $\eta = 1$	Element 25 $\xi = 0.8$ *and* $\xi = 1$ $\eta = 0.8$ *and* $\eta = 1$

Table 6. The node coordinates/control points and knots

Node	Control	Knot	Node	Control	Knot
1	(0,0)	(0,0)	19	(0,30)	(0,0.6)
2	(10,0)	(0.2,0)	20	(10,30)	(0.2,0.6)
3	(20,0)	(0.4,0)	21	(20,30)	(0.4,0.6)
4	(30,0)	(0.6,0)	22	(30,30)	(0.6,0.6)
5	(40,0)	(0.8,0)	23	(40,30)	(0.8,0.6)
6	(50,0)	(1,0)	24	(50,30)	(1,0.6)
7	(0,10)	(0,0.2)	25	(0,40)	(0,0.8)
8	(10,10)	(0.2,0.2)	26	(10,40)	(0.2,0.8)
9	(20,10)	(0.4,0.2)	27	(20,40)	(0.4,0.8)
10	(30,10)	(0.6,0.2)	28	(30,40)	(0.6,0.8)
11	(40,10)	(0.8,0.2)	29	(40,40)	(0.8,0.8)
12	(50,10)	(1,0.2)	30	(50,40)	(1,0.8)
13	(0,20)	(0,0.4)	31	(0,50)	(0,1)
14	(10,20)	(0.2,0.4)	32	(10,50)	(0.2,1)
15	(20,20)	(0.4,0.4)	33	(20,50)	(0.4,1)
16	(30,20)	(0.6,0.4)	34	(30,50)	(0.6,1)
17	(40,20)	(0.8,0.4)	35	(40,50)	(0.8,1)
18	(50,20)	(1,0.4)	36	(50,50)	(1,1)

6.1.2 Knot vector

A knot vector in one-dimension is a set of coordinates in the parametric space $\Xi = \{\xi_1\ \xi_2 \dots\dots\dots \xi_{n+p-1}\ \xi_{n+p}\ \xi_{n+p+1}\} = \{0, 0, 0, 0.2, 0.4, 0.6, 0.8, 1, 1, 1\}$, where ξ_i is the i[th] knot in the Knot vector and p is the order of polynomial and n is the number of basis functions which comprise the B-Spline/NURBS, given weight is equal to one.

6.1.3 Derive the NURBS basis function for element 1

For i = 1 and p = 1

$$N_{1,1}(\xi) = \frac{\xi\ \ -\xi_1}{\xi_2-\xi_1}N_{1,0}(\xi) + \frac{\xi_3-\xi}{\xi_3-\xi_2}N_{2,0}(\xi) = \frac{\xi-0}{0-0}N_{1,0}(\xi) + \frac{0-\xi}{0-0}N_{2,0}(\xi) = 0$$

For i = 2 and p = 1

$$N_{2,1}(\xi) = \frac{\xi\ \ -\xi_2}{\xi_3-\xi_2}N_{2,0}(\xi) + \frac{\xi_4-\xi}{\xi_4-\xi_3}N_{3,0}(\xi) = \frac{\xi-0}{0-0}N_{2,0}(\xi) + \frac{0.2-\xi}{0.2-0}N_{3,0}(\xi) = (1-5\xi)\,N_{3,0}(\xi)$$

For i = 3 and p = 1

$$N_{3,1}(\xi) = \frac{\xi\ \ -\xi_3}{\xi_4-\xi_3}N_{3,0}(\xi) + \frac{\xi_5-\xi}{\xi_5-\xi_4}N_{4,0}(\xi) = \frac{\xi\ \ -0}{0.2-0}N_{3,0}(\xi) + \frac{0.4-\xi}{0.4-0.2}N_{4,0}(\xi)$$

For i = 4 and p = 1

$$N_{4,1}(\xi) = \frac{\xi\ \ -\xi_4}{\xi_5-\xi_4}N_{4,0}(\xi) + \frac{\xi_6-\xi}{\xi_6-\xi_5}N_{5,0}(\xi) = \frac{\xi\ \ -0.2}{0.4-0.2}N_{4,0}(\xi) + \frac{0.6-\xi}{0.6-0.4}N_{5,0}(\xi)$$

For i = 5 and p = 1

$$N_{5,1}(\xi) = \frac{\xi\ \ -\xi_5}{\xi_6-\xi_5}N_{5,0}(\xi) + \frac{\xi_7-\xi}{\xi_7-\xi_6}N_{6,0}(\xi) = \frac{\xi\ \ -0.4}{0.6-0.4}N_{5,0}(\xi) + \frac{0.8-\xi}{0.8-0.6}N_{6,0}(\xi)$$

For i = 6 and p = 1

$$N_{6,1}(\xi) = \frac{\xi\ \ -\xi_6}{\xi_7-\xi_6}N_{6,0}(\xi) + \frac{\xi_8-\xi}{\xi_8-\xi_7}N_{7,0}(\xi) = \frac{\xi\ \ -0.8}{0.8-0.6}N_{6,0}(\xi) + \frac{1-\xi}{1-0.8}N_{7,0}(\xi)$$

For i = 7 and p = 1

$$N_{7,1}(\xi) = \frac{\xi\ \ -\xi_7}{\xi_8-\xi_7}N_{7,0}(\xi) + \frac{\xi_9-\xi}{\xi_9-\xi_8}N_{8,0}(\xi) = \frac{\xi\ \ -1}{1-1}N_{7,0}(\xi) + \frac{1-\xi}{1-1}N_{8,0}(\xi) = 0$$

For i = 8 and p = 1

$$N_{8,1}(\xi) = \frac{\xi\ \ -\xi_8}{\xi_9-\xi_8}N_{8,0}(\xi) + \frac{\xi_{10}-\xi}{\xi_{10}-\xi_9}N_{9,0}(\xi) = \frac{\xi\ \ -1}{1-1}N_{8,0}(\xi) + \frac{1-\xi}{1-1}N_{9,0}(\xi) = 0$$

6.1.4 Gauss points of Integration

For element 1

$$\xi = 0\ and\ \xi = \frac{1}{5};\ \eta = 0\ and\ \eta = \frac{1}{5} \tag{32}$$

The Jacobian is $J_{\bar{\xi},\bar{\eta}} = \frac{1}{4}\,(\xi_{i+1}-\xi_i)(\eta_{i+1}-\eta_i) = \frac{1}{4} * \left(\frac{1}{5}-0\right) * \left(\frac{1}{5}-0\right) = \frac{1}{100}$

Parent element Gauss Points of Integration are $\pm\frac{1}{\sqrt{3}}, \pm\frac{1}{\sqrt{3}}$

Parametric space $\frac{1}{2}\left[(\xi_{i+1}-\xi_i)\hat{\xi} + (\xi_{i+1}-\xi_i)\right] = \frac{1}{2}\left[\left(\frac{1}{5}-0\right)\left(\frac{1}{\sqrt{3}}\right) + \left(\frac{1}{5}-0\right)\right] = 0.157735 = \frac{1}{2}\left[\left(\frac{1}{5}-0\right)\left(\frac{-1}{\sqrt{3}}\right) + \left(\frac{1}{5}-0\right)\right] = 0.04226497$

The parametric to physical space.
Gauss points of Integration are (0.157735, 0.157735) (0.157735, 0.0422649) (0.0422649, 0.157735) (0.0422649, 0.0422649).
The Isoparametric formulation is given in Appendix A.

7. Isogeometric Sizing Optimization

In this section, the sizing optimization of a beam is performed using Isogeometric analysis.

7.1 Isogeometric Optimal Cross Section Dimensions of a Beam Carrying Point Load

A cantilever is fixed at the left end and free at the right end as shown in Fig.5. It carries a point load of magnitude P equal to 100 kN acting vertically downwards. The length of the cantilever beam is equal to 1000 mm. The Young's modulus of elasticity of the material is 200 GPa and the initial cross-section is circular and having a radius of 103.4630 mm over the entire length of the beam. The moment of inertia is 90033662.5464988 mm^4. The weight density of the material is 78700 N/m^3. The total number of control points is 101, and the number of elements is 98. The number of control points for each element is four. The number of control points which are in common for every two elements are equal to three which concludes that the beam satisfies C^2 connectivity. The degree of the polynomial is equal to three.
The length of the knot vector Xi is 105. The knot vector is given by

Xi Vector = {0 0 0 0 10.20408163 20.40816327 30.6122449 40.81632653
51.02040816 61.2244898 71.42857143 81.63265306 91.83673469 102.0408163
112.244898 122.4489796 132.6530612 142.8571429 153.0612245 163.2653061
173.4693878 183.6734694 193.877551 204.0816327 214.2857143 224.4897959
234.6938776 244.8979592 255.1020408 265.3061224 275.5102041 285.7142857
295.9183673 306.122449 316.3265306 326.5306122 336.7346939 346.9387755
357.1428571 367.3469388 377.5510204 387.755102 397.9591837 408.1632653
418.3673469 428.5714286 438.7755102 448.9795918 459.1836735 469.3877551
479.5918367 489.7959184 500 510.2040816 520.4081633 530.6122449
540.8163265 551.0204082 561.2244898 571.4285714 581.6326531 591.8367347
602.0408163 612.244898 622.4489796 632.6530612 642.8571429 653.0612245
663.2653061 673.4693878 683.6734694 693.877551 704.0816327 714.2857143
724.4897959 734.6938776 744.8979592 755.1020408 765.3061224 775.5102041
785.7142857 795.9183673 806.122449 816.3265306 826.5306122 836.7346939
846.9387755 857.1428571 867.3469388 877.5510204 887.755102 897.9591837
908.1632653 918.3673469 928.5714286 938.7755102 948.9795918 959.1836735
969.3877551 979.5918367 989.7959184 1000 1000 1000 1000}

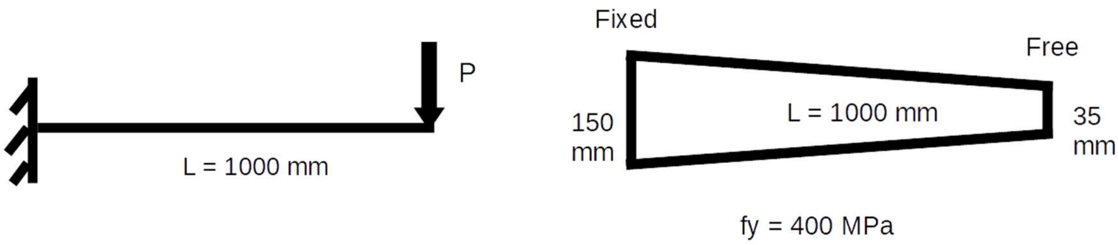

(a) (b)

Fig. 5. (a) Cantilever beam carrying a point load at the free end, and (b) optimized cross-section dimensions of the Cantilever beam

7.1.1 Discussion of results

The analytical expression to find the deflection at x measured from free end is given by Macaulay's method. The deflection at any section is given by

$$EI\,y = -\left[\frac{Wlx^2}{2} - \frac{Wx^3}{6}\right] \tag{33}$$

Two nodes at the left end are fixed. The vertical deflection at these two nodes is set to zero. The analytical solution to find the deflection under the load is given by

$$-\,WL^3/(3EI) = -\frac{100000*(990^3)}{(200000*90033662.5464988*3)} = -1.79618\text{ mm} \tag{34}$$

The transverse vertical deflection curve of the cantilever beam with left end fixed which carries a point load acting vertically downwards the free end on the right is as shown in Fig. 6. The Global stiffness matrix and global force vector are assembled. The nodal displacements are calculated. The nodal displacement calculated using Isogeometric analysis are similar to the nodal displacements obtained using analytical expressions.

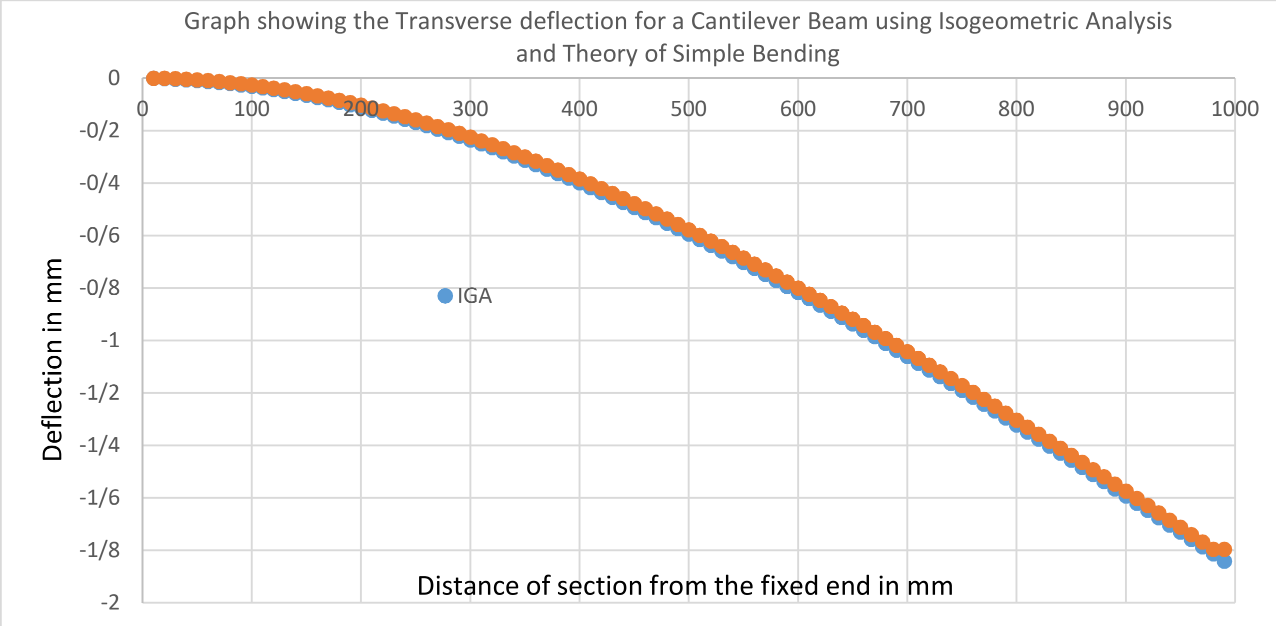

Fig. 6. The deflected curve of the cantilever beam carrying point load at the free end on the right

Table 7. The vertical deflection at different points along the length of the beam

Deflection	Using Isogeometric Analysis	Using Analytical Expression	Ratio IGA/Analytical
At the free end	-1.84116 mm	-1.79618 mm	1.02504

The results show that the transverse deflection calculated using the Isogeometric analysis is nearly equal to the deflection achieved using analytical Macaulay's method. The results show that the maximum deflection obtained using IGA is 2.504% higher than the maximum deflection calculated analytically.

7.1.2 Optimal cross section

The stress at the centroid of each element is calculated using Isogeometric analysis, the optimal cross section dimensions are then determined. The optimal cross section dimensions are also determined using the theory of simple bending as well. The results are then compared and are tabulated. The formulation to calculate the stress is given below in 7.1.2.1. The stress at the centroid of each element is tabulated as shown in the Table 8.

7.1.2.1 Compute Maximum Stress using IGA

As shown in the Fig. 7a and 7b the cantilever is fixed at left end and carries a point load P at the free end on the right. The cross section is circular and the deflected curve at any point shows that the axial displacement is denoted by U_{xx} and the vertical transverse displacement is z. The angle made by the tangent to the deflected curve with the vertical is *w'*.

$$slope\ w' = \frac{u_{xx}}{z} \tag{35}$$

$$strain\ \in = \frac{du_{xx}}{dx} = y\, w''\ (where\ the\ distance\ measure\ z = y) \tag{36}$$

$$w'' = \frac{d^2w}{dx^2} = \frac{\sum_i\ d^2N_i}{dx^2} z_i \tag{37}$$

$$w = \sum_{i=1}^{n} N_i(\xi) z_i\,, where\ N_i\ is\ the\ B - Splines/NURBS\ polynomial\ of\ degree\ p \tag{38}$$

$$\frac{dN}{d\xi} = \frac{dN}{dx}\frac{dx}{d\xi} = J\frac{dN}{dx} \tag{39}$$

$$\frac{d^2N}{d\xi^2} = \left(\frac{d}{d\xi}\left(\frac{dN}{dx}\right)\right)\left(\frac{dx}{d\xi}\right) + \frac{dN}{dx}\frac{d^2x}{d\xi^2} = \left(\frac{d^2N}{dx^2}\right)\left(\frac{dx}{d\xi}\right)\left(\frac{dx}{d\xi}\right) + \left(\frac{dN}{dx}\right)\left(\frac{d^2x}{d\xi^2}\right) \tag{40}$$

$$\frac{d^2N_i}{dx^2} = \frac{1}{J^2}\left[\frac{d^2N_i}{d\xi^2} - \left(\frac{1}{J}\right)\left(\frac{dN_i}{d\xi}\right)\left(\frac{d^2x}{d\xi^2}\right)\right] \tag{41}$$

$$strain = y\, w'' = y\left(\sum_i \frac{d^2N_i}{dx^2} z_i\right) \tag{42}$$

$$x = \sum_i N_i(\xi)x_i \ and \ \frac{d^2x}{d\xi^2} = \sum_i \frac{d^2N_i}{d\xi^2}x_i \tag{43}$$

$$stress = E * strain \tag{44}$$

where y is the distance to the most distant fibre from neutral axis in the cross section and the z_i are the nodal transverse vertically downward deflection. The stress is measured at the centroid of each element knot span. The diameter of the bar is 206.92747 *mm*, and the maximum stress at the support is 150.38 N/mm^2 as shown in Table 8. The results show that stresses obtained using the Isogeometric analysis are similar to stresses acquired by theory of simple bending as shown in the Fig.7c. The stress evaluation using Isogeometric analysis displays that at the support the variation of stress is not linear and at sections far away from the support the variation of the stress is found to be linear.

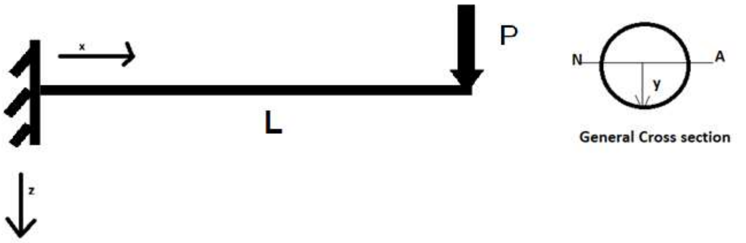

(a)

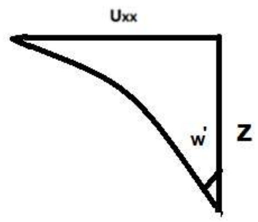

(b)

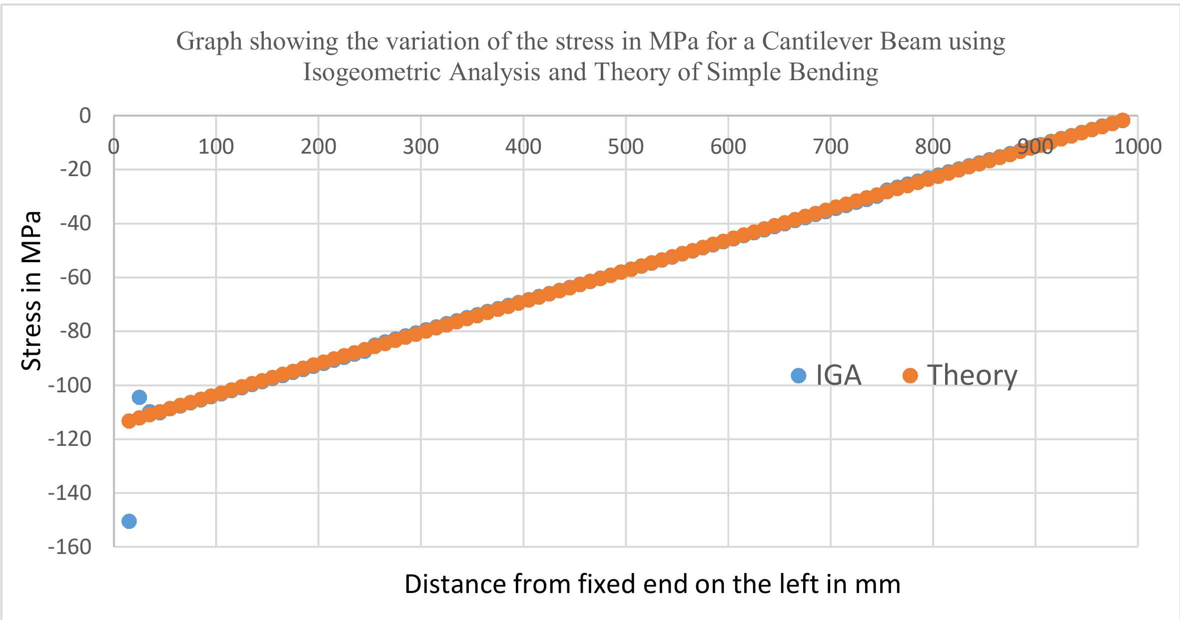

(c)

Fig. 7. (a) Cantilever beam and the cross-section (b) The curvature of the deflected beam over an elementary length and (c) The variation of stress in MPa for a Cantilever beam using IGA and Simple Bending

The maximum permissible stress of the material is equal to 400 MPa.

The diameter of the bar at the left end is equal to $(\frac{150.38}{400} * 8 * 103.463^3)^{1/3}$ = 149.345 mm

The diameter of the bar at the right end is equal to $(\frac{1.81587}{400} * 8 * 103.463^3)^{\frac{1}{3}}$ = 34.2628 mm

The diameter of the circular beam rounded to the nearest integer is equal to 150 mm at the fixed support on the left end and linearly varying to 35 mm at the free end on the right end as shown in the Fig.5b.

7.1.2.2 Cross section using theory of simple bending

The cross section is determined using the bending stress criteria and shear stress criteria.

Using Bending stress criteria

The diameter of the bar at the left end is equal to = $(\frac{113.192}{400} * 8 * 103.463^3)^{1/3}$ = 135.852 mm

The diameter of the bar at the right end is equal to = $(\frac{1.7237}{400} * 8 * 103.463^3)^{1/3}$ = 33.6733 mm

Using Shear stress criteria

The shear force is constant throughout the length of the beam. The maximum shear stress is given by 4/3 the average shear stress.

The area of the cross section is 33643.0045882857 mm^2

Maximum shear stress is given by 4×100000/(3×33643.0045882857) = 3.963181 MPa

Maximum permissible shear stress is = (400-0)/2 = 200 MPa

The radius of the cross section for the beam is equal to $(\frac{3.963181}{200} * 103.463^2)^{1/2}$ = 14.56 mm

The diameter of the cross section for the beam using shear stress criteria is equal to 29.12 mm.

Table 8. The stress at the centroid of each element using IGA and theory of simple bending

Distance Mm	IGA MPa	Theory MPa	IGA/Theory	Dist mm	IGA MPa	Theory MPa	IGA/Theory
15	-150.38	-113.1921685	1.3285371	505	-56.8949	-56.88337401	1.0002026
25	-104.475	-112.0430094	0.9324544	515	-55.7687	-55.73421494	1.0006187
35	-109.809	-110.8938503	0.9902172	525	-54.6425	-54.58505587	1.0010524
45	-110.178	-109.7446913	1.0039483	535	-53.5163	-53.4358968	1.0015047
55	-108.629	-108.5955322	1.0003082	545	-52.3902	-52.28673773	1.0019787
65	-107.622	-107.4463731	1.0016346	555	-51.264	-51.13757865	1.0024722
75	-106.462	-106.2972141	1.0015502	565	-50.1378	-49.98841958	1.0029883
85	-105.345	-105.148055	1.001873	575	-49.0116	-48.83926051	1.0035287
95	-104.217	-103.9988959	1.0020972	585	-47.8855	-47.69010144	1.0040973
105	-103.091	-102.8497368	1.0023458	595	-46.7593	-46.54094237	1.0046917
115	-101.965	-101.7005778	1.0026	605	-45.6331	-45.3917833	1.0053163
125	-100.839	-100.5514187	1.00286	615	-44.5069	-44.24262423	1.0059733
135	-99.7125	-99.40225963	1.0031211	625	-43.3808	-43.09346516	1.0066677
145	-98.5864	-98.25310056	1.0033923	635	-42.2546	-41.94430609	1.0073978
155	-97.4602	-97.10394149	1.0036688	645	-41.1284	-40.79514702	1.0081689
165	-96.334	-95.95478242	1.003952	655	-40.0022	-39.64598795	1.0089848
175	-95.2078	-94.80562335	1.0042421	665	-38.8761	-38.49682887	1.009852
185	-94.0817	-93.65646428	1.0045404	675	-37.7499	-37.3476698	1.0107699
195	-92.9555	-92.50730521	1.004845	685	-36.6237	-36.19851073	1.011746
205	-91.8293	-91.35814614	1.0051572	695	-35.4975	-35.04935166	1.0127862
215	-90.7031	-90.20898706	1.0054774	705	-34.3713	-33.90019259	1.0138969
225	-89.5769	-89.05982799	1.0058059	715	-33.2452	-32.75103352	1.0150886
235	-88.4508	-87.91066892	1.0061441	725	-32.119	-31.60187445	1.0163638
245	-87.3246	-86.76150985	1.0064901	735	-30.9928	-30.45271538	1.0177352
255	-85.0493	-85.61235078	0.9934233	745	-29.8666	-29.30355631	1.0192142
265	-83.9231	-84.46319171	0.9936056	755	-27.5913	-28.15439724	0.9799997
275	-82.7969	-83.31403264	0.993793	765	-26.4651	-27.00523817	0.9799988
285	-81.6707	-82.16487357	0.9939856	775	-25.339	-25.85607909	0.9800016
295	-80.5446	-81.0157145	0.9941849	785	-24.2128	-24.70692002	0.9800007
305	-79.4184	-79.86655543	0.9943887	795	-23.0866	-23.55776095	0.9799998
315	-78.2922	-78.71739636	0.9945984	805	-21.9604	-22.40860188	0.9799987
325	-77.166	-77.56823728	0.9948144	815	-20.8343	-21.25944281	0.9800022
335	-76.0399	-76.41907821	0.9950382	825	-19.7081	-20.11028374	0.9800011
-345	-74.9137	-75.26991914	0.9952674	835	-18.5819	-18.96112467	0.9799999
355	-73.7875	-74.12076007	0.9955038	845	-17.4557	-17.8119656	0.9799985
365	-72.6613	-72.971601	0.9957476	855	-16.3296	-16.66280653	0.980003
375	-71.5352	-71.82244193	0.9960007	865	-15.2034	-15.51364746	0.9800016
385	-70.409	-70.67328286	0.9962605	875	-14.0772	-14.36448839	0.9800001
395	-69.2828	-69.52412379	0.9965289	885	-12.951	-13.21532932	0.9799983
405	-68.1566	-68.37496472	0.9968064	895	-11.8249	-12.06617024	0.9800044
415	-67.0304	-67.22580565	0.9970933	905	-10.6986	-10.91701117	0.9799935
425	-65.9043	-66.07664658	0.9973917	915	-9.57265	-9.767852102	0.9800159
435	-64.7781	-64.9274875	0.9976992	925	-8.44578	-8.618693032	0.9799374
445	-63.6519	-63.77832843	0.9980177	935	-7.32206	-7.469533961	0.9802566
455	-62.5257	-62.62916936	0.9983479	945	-6.18716	-6.32037489	0.9789229
465	-61.3996	-61.48001029	0.9986921	955	-5.09194	-5.171215819	0.9846698
475	-60.2734	-60.33085122	0.9990477	965	-3.85626	-4.022056748	0.9587781
485	-59.1472	-59.18169215	0.9994172	975	-2.82749	-2.872897677	0.9841945
495	-58.021	-58.03253308	0.9998013	985	-1.81587	-1.723738606	1.0534486

7.1.2.3 Summary of the cross section dimensions determined using IGA and Simple Bending

The summary of the cross section dimensions of the beam determined using Isogeometric analysis and by applying the Theory of Simple Bending are as shown in the Table 9 below.

Table 9. Summary of optimal cross section dimensions in mm for the Cantilever beam determined using IGA and Theory of Simple Bending

	IGA	Theory of Simple Bending		Optimal
		Bending Stress	Shear Stress	
Diameter at left end	149.345	135.852	29.12	149.345
Diameter at right end	34.2628	33.6733	29.12	34.2628

The obtained stress using Isogeometric analysis is similar to the stress calculated using theory of simple bending. The optimal dimensions of the cross section are as shown in the Fig.5b.

8. Isogeometric Topology Optimization of Continuum Structures

In this section, two examples are solved. In section 8.1, we present a two dimensional simply supported plate carrying a point load at the center, also known as Michelle structure. In section 8.2, a three dimensional simply supported cube domain carrying a point load at the center is optimized and presented.

8.1 Two-Dimensional Structure

A two-dimensional plate structure is optimized in this section as follows.

8.1.1 A Simply supported beam carrying a point load at the center of the lower edge between the supports (Michelle)

The given design domain is a simply supported beam 9600×3300 mm. The beam carries a point load (P) of magnitude 10056 N at the center. For the sake of simplicity, half of the domain is analyzed due to symmetry. The mesh consists of 352 elements and 396 control points. The modulus of Elasticity is taken as 2×10^5 N/mm^2 and the Poisson's ratio is as 0.3. The weight density is 7870 kg/m^3. The thickness is one unit. The degree of basis function is one along each direction. The design domain is as shown in the Fig.8. Only one half of the design domain is optimized due to symmetry. Fig. 9(a) shows the optimal distribution of material using the firefly algorithm. The design is a fully stressed design. Fig. 9(b) displays the optimal distribution and is compared with the optimal distribution of Hassani (2012) using 1617 control points. Table 16 shows the comparison of the minimum volume obtained by Firefly algorithm and those of Hassani et. al. (2012). The final weight of the structure is higher. The number of elements which are used is few and the element size is large. Hence, the weight of the final distribution is slightly over.

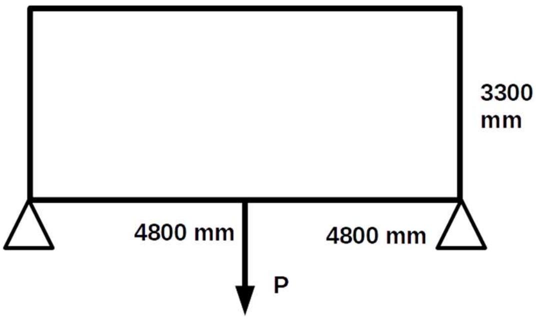

Fig. 8. The initial design domain of a simply supported plate

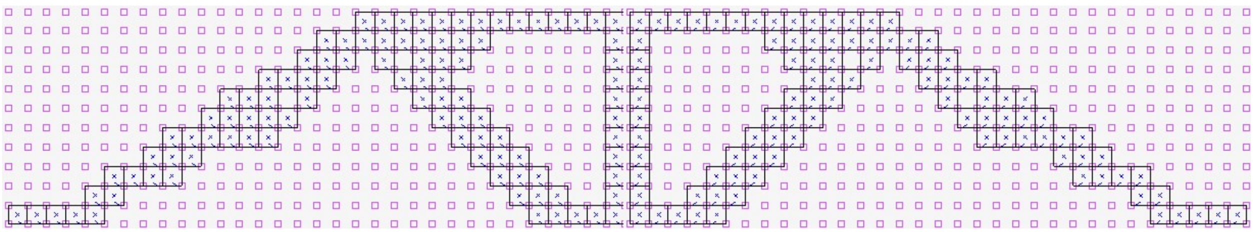

(a)

(b)

Fig. 9. (a) The optimal distribution for the entire beam which is symmetrical about the center using 396 control points (b) Optimal distribution, 1617 ctrl pts (Hassani, 2012)

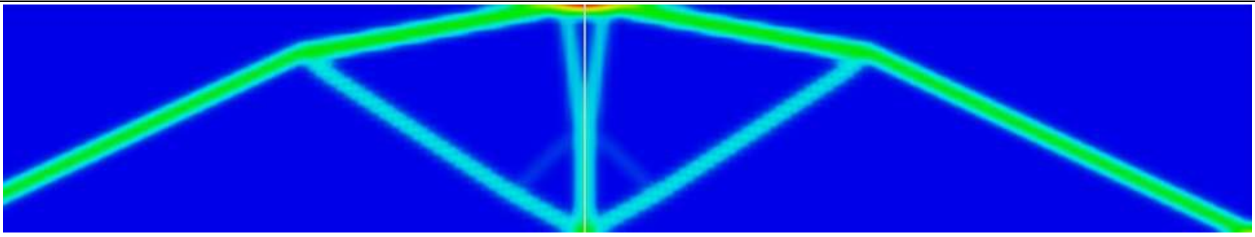

Fig. 10. The distribution of material within the design domain of the Michelle structure using a Standard Finite Element Analysis Package MIDAS NFX® by first-order four-node quadrilateral elements

Table 10. Comparison of the volume fraction for a simply supported beam

	Hassani et. al. (2012)	Present study using FFA-IGA (2018)
Number of control points	1617	396
Minimum Volume (V/V_0)	20%	27.84 %
Number of Elements	1600	352

As shown in the Table 10, the minimum volume obtained after optimisation using IGAFFA is 27.84% when compared with the minimum volume of the optimal distribution by Hassani (2012) is 20%. The optimal distribution of material is in good agreement with the optimal distribution by Hassani (2012) and the optimal distribution arrived by using MIDAS NFX® a commercial package as shown in the Fig.10. One half of the domain is analysed due to symmetry.

8.2 Three dimensional Structure

A three dimensional structure is optimized in this section as follows.

8.2.1 A simply supported three dimensional cube carrying a point load at the centre on the top face

The design domain is a three dimensional cube domain having equal sides of 5m each. The bottom four corners are simply supported and the center of the top face carries a point load (P) of 1000 N acting vertically upwards. The domain is meshed using 1000 first order eight node hexahedral elements. The total number of control points are 1331. The modulus of elasticity of the material is taken as 1e5 MPa and the Poisson's ratio as 0.3.
The knot vector is [0, 0, 0, 0.1, 0.2, 0.3, 0.4, 0.5, 0.6, 0.7, 0.8, 0.9, 1, 1, 1] along each direction X, Y and Z and the length of the knot vector is 15. The degree of the NURBS curve is equal to one along each direction.

Table 11. Comparison of the weight of the final optimal distribution of material

	Abolbashari using FEA(2006)	This study using IGAFFA (2018)
%Volume reduction	82.4	88.5
Final volume (V/V_0)	17.6%	11.5%
Number of Iterations	-	196

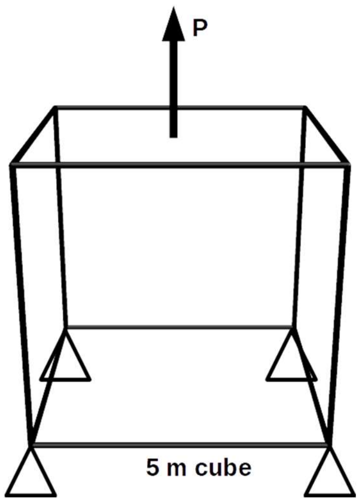

Fig. 11. The initial three-dimensional design domain.

The number of iterations is 196. The number of elements carrying the material at the optimum is equal to 115 out of a total of 1000 in the solid domain, 11.5% of the initial domain.
A similar problem has been solved by Abolbashari in 2006. He used 1000 elements, 8 nodes, first-order hexahedral elements and performed finite element analysis for three-dimensional solid continuum.
In this study, the results (Table 11) achieved using Isogeometric analysis can be compared with those results found by Abolbashari (2006) using Finite element analysis. The volume of material saved 88.5% of the initial volume by using IGA when compared with 82.4% of material saved using FEA. The final volume hiring IGAFFA is 11.5% of the initial volume which is lower when compared to the final volume attained by Abolbashari by FEA which is 17.6%.

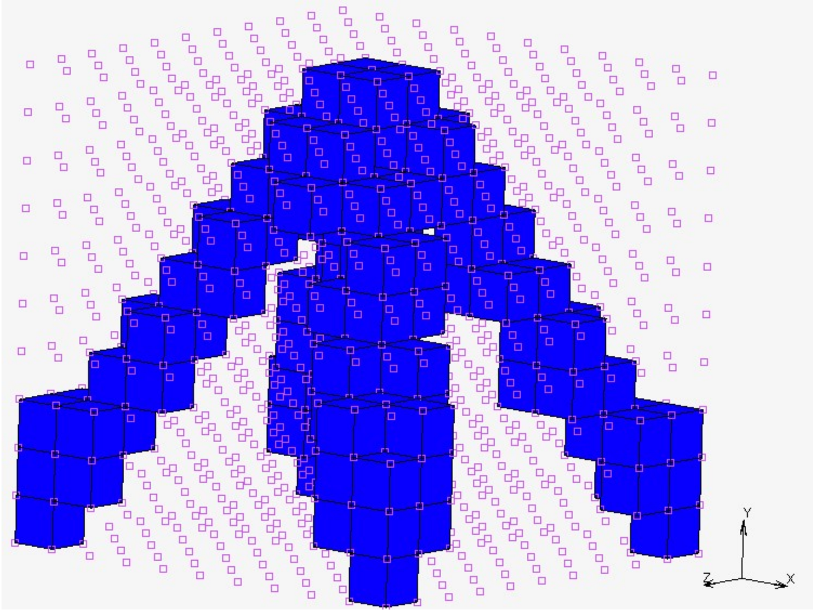

Fig. 12. The optimal distribution of material for 3D continuum.

9. Conclusions

The objective of this study is to apply the Isogeometric analysis which is the next generation method to perform structural analysis. The basic governing equations are presented in the theoretical background. The basic problems in civil engineering are analyzed using Isogeometric analysis. The plate carrying in-plane loading is solved first by using B-splines with its degree equal to one. This section clearly explains a step by step procedure on how to derive the basis functions, and derives the stiffness matrix for the plate. form the global stiffness matrix and determining the nodal displacements for each node. The found nodal displacements using the Isogeometric analysis are then compared with the nodal displacements determined by utilizing a standard finite element analysis package MARC Mentat ®. The results clearly show that the achieved displacements by both of these methods are in good agreement.

Also, the problems of sizing optimization of the beam are solved. A cantilever beam carrying a point load acting vertically downwards at the free end is taken and the governing equations to determine the stresses at any point along the length of the beam are then derived. The governing equations are then solved using NURBS and the stresses are then determined. The cross sectional areas are then determined at the optimal point. The bending stress criteria and shear stress criteria are also verified as well. The final cross section dimensions are then determined for the beam. The diameter of the circular cross section of a beam is 149.345 mm at the left end and varies linearly to 34.2628 mm under the load at the free end on the right.

Topology optimization of continuum structures is performed. The plate problems carrying an in-plane loading are optimized using the evolutionary algorithm. In this study, the firefly algorithm is used which is proposed by XS Yang. It is based on the fireflies searching for food. The Firefly algorithm is one of the best algorithms to locate the optimal point. In this study, one problem in two-dimensional domain is optimized and one problem in three-dimensional domain is optimized. In the two-dimensional domain, a simply supported beam carrying a point load at the center of the bottom edge in between the supports (Michelle beam) is optimized. The optimal distribution is also solved using MIDAS NFX® an independent standalone commercial package as well. The optimal distribution of the material is similar in all three cases. The simply supported beam is optimized using 396 control points. For the sake of symmetry, only one half of the beam is analyzed. Hassani et al. (2012) optimized a similar structure using 1617 control points. The volume of the material at optimization situation is 27.84% in this study as compared to 20% of initial volume achieved by Hassani et al. The found results are in good agreement with the previous acquired results in the literature. A three-dimensional problem is solved by B-Splines with degree equal to one along three directions. The volume of the optimal structure is then compared with the achieved results in the existing literature. The three-dimensional problem is optimized by Abolbashari in 2006 using first-order eight node hexahedral elements. The acquired final volume by Abolbashari (2006) is 17.6% of the initial volume as compared to 11.5% of the initial volume in this study using Isogeometric analysis. The results show that the optimal distribution found by using Isogeometric analysis is more efficient than other methods.

This study has proven that the Isogeometric analysis (IGA) can be effectively and efficiently used to solve the problems in structural mechanics. The basic advantage of using IGA is to derive the basis functions from the geometry and the same basis functions are used to derive the displacements as well. The geometry can be accurately represented using NURBS and hence the results are more accurate over finite element analysis (FEA). We hope this study can be useful to learn and understand the concept of Isogeometric analysis and its applications in civil engineering domain.

The study can be further extended to apply the Isogeometric analysis to optimize shell structures.

- The current study is focused on using NURBS basis functions, in future T-splines can be used instead.
- The study can be extended to include non-linear analysis and a few optimization problems including fracture mechanics can be addressed as well.

Acknowledgments

We acknowledge everyone whose incessant support and enthusiasm has helped us to complete and review the paper.

Conflict of Interest

The author(s) declared no potential conflicts of interest with the research, authorship and publication of this article.

Funding

The author(s) received no financial support for the research, authorship and publication of this article.

References

[1] Archana, B., Chandrasekhar, K.N.V., A Study on Parameters of Firefly Algorithm for Topology Optimisation of Continuum Structures – II", *i-manager's Journal on Structural Engineering* 6(1) (2017) 16-27.
[2] Clough, R.W., Penzien J., *Dynamics of Structures, Computers and Structures*, 2nd edition, 2010.
[3] Gondegaon S, Voruganti H., Static Structural and Modal Analysis Using Isogeometric Analysis, *Journal of Theoretical and Applied Mechanics* 46(4) (2106) 36–75.
[4] Gondegaon, S., Ahmada, R. & Voruganti, H. K., *Geometric Modeling For Isogeometric Analysis*, Proceedings of ICTACEM 2014 International Conference on Theoretical, Applied, Computational and Experimental Mechanics, 2014.
[5] Hartman et.al., *About Isogeometric analysis and the new NURBS-based Finite elements in LS-DYNA*, 8th European LS-DYNA Users Conference, May 23-24, Strasbourg, France, 2011.
[6] Hassani et. el., An Isogeometric approach to structural topology optimization by optimality criteria, *Struct. Multidisc. Optim.* 45 (2012) 223–233.
[7] Hughes T.J.R., et al., Isogeometric Analysis: CAD, Finite Elements, NURBS, Exact Geometry and Mesh Refinement, *Comput. Methods in Appl. Mech. Eng.* 194 (2005) 4135–4195.
[8] De Lorenzis, L., Some recent issues and open issues on interface modelling in Civil Engineering Structures, *Materials and Structures* 45 (2012) 477-503.
[9] Espath, L.F.R., Braun, A.L., & Awruch, A.M., An Introduction To Isogeometric Analysis Applied To Solid Mechanics, *Mecánica computacional* 30 (2011) 1955-1975.
[10] Lee, J. S., An, Y. N., & Chang, K., *Optimum structural design based on isogeometric analysis method*, In Strategic Technology (IFOST), 2010 International Forum on, October, 2010.
[11] Bendsoe, M.P., Sigmund, O., Material interpolation schemes in topology optimization, *Archive of Applied Mechanics* 69 (1999) 635-654.
[12] Hsu, M.H., Hsu, Y.L., Generalization of two- and three dimensional structural topology optimization, *Engineering Optimization* 37 (2005a) 83-102.
[13] Hsu, M.H., Hsu, Y.L., Interpreting three-dimensional structural topology optimization results, *Computers and Structures* 83(4–5) (2005) 327-337.
[14] Abolbashari, M.H., Keshavarzmanesh, Sh., On various aspects of application of the evolutionary structural optimization method for 2D and 3D continuum structures, *Finite Elements in Analysis and Design* 42 (2006) 478–491.
[15] Rauen, M., et. al., *Isogeometric analysis of free vibration of bars*, 22nd International Congress of Mechanical Engineering, November 3-7, SP, Brazil, 2013.
[16] Jockovic, M., *Free vibration analysis of beam element using Isogeometric analysis*, 4th International conference on Contemporary achievements in Civil Engineering, 22nd April, Serbia, 2016.
[17] Shah, M., Katukum, R., *Stress analysis without meshing Isogeometric analysis finite element method*, UG Summer Internship, Boeing, India, International Conference on Innovations in Computer Science and Technology, ICICSIT, 2015.
[18] Shah, M., Katukam, R., *Stress Analysis Without Meshing Iso-Geometric Analysis Finite Element Method (IGAFEM)*, Boeing Summer Internship Project, 2015.
[19] Attila, N., et. al., On the variation formulation of stress constraints in Isogeometric design, *Computational Methods in Applied Mechanics and Engineering* 199 (2010) 2687-2696.
[20] Valizadeh, N., Ghorashi, S.S., Mohammadi, S., Shojaee, S., Ghasemzadeh, H., An Improved Isogeometric Analysis Using the Lagrande Multiplier Method, *European Conference on extended finite element*, June 29-30 to July1, 2011.
[21] Ohsaki, M., Swan, C.C., Topology and geometry optimization of trusses and frames, *Recent Advances in Optimal Structural Design* 5 (2002) 97–123.
[22] Reddy, A.A., Kumar, C.N., Reddy, K.A., Chandrasekhar, K.N.V., Optimisation of Steel Transmission Tower Structure Using Firefly Algorithm, *i-manager's Journal on Structural Engineering*, 6(2) (2017) 9-19.
[23] Nguyen, V.P., Bordasa, S.P.A., Rabczuk, T., Isogeometric Analysis: An Overview and Computer Implementation Aspects, *Mathematics and Computers in Simulation* 117 (2015) 89-116.
[24] Yang, X.-S., *Firefly algorithm, Levy flights and global optimization*, Research and Development in Intelligent Systems XXVI (Eds M. Bramer, R. Ellis, M. Petridis), Springer London, pp. 209-218, 2010.

[25] Yang, X.-S., Firefly algorithms for multimodal optimization, Stochastic Algorithms: Foundations and Applications, *Lecture Notes in Computer Sciences* 5792 (2009) 169-178.
[26] Yang, X.S., Swarm intelligence based algorithms: a critical analysis, *Evolutionary Intelligence* 7(1) (2014) 17–28.
[27] Hsu, Y.H., Hsu, M.S., Chen, C.T., Interpreting results from topology optimisation using density contours, *Computers and Structures* 79 (2001) 1049-1058.
[28] Weisse, T., *Global Optimization Algorithms – Theory and Applications*, 2nd Edition, 2008. http://www.it-weise.de

APPENDIX A: Isogeometric Formulation

A.1 Isogeometric Formulation

NURBS basis functions are used to represent the geometry and also the displacement at any point within the element. Hence, the formulation is also known as 'Iso' (which means the same) 'geometric' (here NURBS basis functions) based formulation. The displacement at any point in the element expressed in terms of nodal displacements is given by

$$\begin{aligned} U &= N_1M_1U_1 + N_2M_1U_3 + N_2M_2U_5 + N_1M_2U_7 \\ V &= N_1M_1U_2 + N_2M_1U_4 + N_2M_2U_6 + N_1M_2U_8 \end{aligned} \tag{A1}$$

The co-ordinates of any point in the element expressed in terms of the nodal co-ordinates is given by

$$\begin{aligned} X &= N_1M_1X_1 + N_2M_1X_2 + N_2M_2X_3 + N_1M_2X_4 \\ Y &= N_1M_1Y_1 + N_2M_1Y_2 + N_2M_2Y_3 + N_1M_2Y_4 \end{aligned} \tag{A2}$$

A.1.1 Derivative of NURBS basis function

The basis functions are

$$\begin{gathered} N_1 = (1-5\xi) and\ N_2 = 5\xi\ and\ M_1 = (1-5\eta) and\ M_2 = 5\eta \\ \frac{\partial(N_1M_1)}{\partial\xi} = (-5)(1-5\eta)\ and\ \frac{\partial(N_2M_1)}{\partial\xi} = (5)(1-5\eta) \\ \frac{\partial(N_2M_2)}{\partial\xi} = (5)(5\eta)\ and\ \frac{\partial(N_1M_2)}{\partial\xi} = (-5)(5\eta) \\ \frac{\partial(N_1M_1)}{\partial\eta} = (-5)(1-5\xi)\ and\ \frac{\partial(N_2M_1)}{\partial\eta} = (5\xi)(-5) \\ \frac{\partial(N_2M_2)}{\partial\eta} = (5)(5\xi)\ and\ \frac{\partial(N_1M_2)}{\partial\eta} = (1-5\xi)(5) \end{gathered} \tag{A3}$$

The Jacobian in parent space is given by

$$\begin{bmatrix} \frac{\partial x}{\partial\xi} & \frac{\partial y}{\partial\xi} \\ \frac{\partial x}{\partial\eta} & \frac{\partial y}{\partial\eta} \end{bmatrix} = \begin{bmatrix} 50 & 0 \\ 0 & 50 \end{bmatrix} \tag{A4}$$

The co-ordinates are given by $X_1 = 0$ $X_2 = 10$ $X_3 = 10$ $X_4 = 0$, $Y_1 = 0$ $Y_2 = 0$ $Y_3 = 10$ $Y_4 = 10$.

A.1.1.1 Derive the Stiffness matrix at integration point (0.157735, 0.0422649)

$$\frac{\partial x}{\partial\xi} = \frac{\partial}{\partial\xi}(N_1M_1X_1 + N_2M_1X_2 + N_2M_2X_3 + N_1M_2X_4) \tag{A5}$$

$$\frac{\partial x}{\partial\xi} = (-5)(1-5*0.0422649)(0) + (5)(1-5*0.0422649)*10 + (5)(5*0.0422649)*10 + (5)(-5*0.0422649)*(0) = 50 \tag{A6}$$

$$\frac{\partial y}{\partial\xi} = \frac{\partial}{\partial\xi}(N_1M_1Y_1 + N_2M_1Y_2 + N_2M_2Y_3 + N_1M_2Y_4) \tag{A7}$$

$$\frac{\partial y}{\partial\xi} = (-5)(1-5*0.0422649)(0) + (5)(1-5*0.0422649)*0 + (5)(5*0.0422649)*10 + (5)(-5*0.0422649)*(10) = 0 \tag{A8}$$

$$\frac{\partial x}{\partial\eta} = \frac{\partial}{\partial\eta}(N_1M_1X_1 + N_2M_1X_2 + N_2M_2X_3 + N_1M_2X_4) \tag{A9}$$

$$\frac{\partial x}{\partial\eta} = (-5)(1-5*0.157735)(0) + (5*0.157735)(-5)(10) + (5)(5*0.157735)*10 + (1-5*0.157735)(5)*0 = 0 \tag{A10}$$

$$\frac{\partial y}{\partial\eta} = \frac{\partial}{\partial\eta}(N_1M_1Y_1 + N_2M_1Y_2 + N_2M_2Y_3 + N_1M_2Y_4) \tag{A11}$$

$$\frac{\partial y}{\partial \eta} = (-5)(1-5*0.157735)(0) + (5*0.157735)(-5)(0) + (5)(5*0.157735)*10 + (1-5*0.157735)(5)*10 = 50 \tag{A12}$$

The strain displacement matrix is

$$B = \begin{bmatrix} \frac{\partial N}{\partial x} & 0 \\ 0 & \frac{\partial N}{\partial y} \\ \frac{\partial N}{\partial y} & \frac{\partial N}{\partial x} \end{bmatrix} \tag{A13}$$

$$\frac{\partial N}{\partial \xi} = \frac{\partial N}{\partial x}\frac{\partial x}{\partial \xi} + \frac{\partial N}{\partial y}\frac{\partial y}{\partial \xi}, \quad \frac{\partial N}{\partial \eta} = \frac{\partial N}{\partial x}\frac{\partial x}{\partial \eta} + \frac{\partial N}{\partial y}\frac{\partial y}{\partial \eta} \tag{A14}$$

$$\begin{bmatrix} \frac{\partial N}{\partial x} \\ \frac{\partial N}{\partial y} \end{bmatrix} = \begin{bmatrix} \frac{\partial x}{\partial \xi} & \frac{\partial y}{\partial \xi} \\ \frac{\partial x}{\partial \eta} & \frac{\partial y}{\partial \eta} \end{bmatrix}^{-1} \begin{bmatrix} \frac{\partial N}{\partial \xi} \\ \frac{\partial N}{\partial \eta} \end{bmatrix} \tag{A15}$$

where N is the basis function matrix $= [\, N_1M_1 \;\; N_2M_1 \;\; N_2M_2 \; N_1M_2]^T$

$$strain\ \varepsilon = \left[\frac{\partial u}{\partial x}, \frac{\partial v}{\partial y}, \frac{\partial u}{\partial y} + \frac{\partial v}{\partial x}\right]^T \tag{A16}$$

$$\begin{bmatrix} \frac{\partial u}{\partial x} \\ \frac{\partial u}{\partial y} \end{bmatrix} = \frac{1}{|J|} \begin{bmatrix} J_{22} & -J_{12} \\ -J_{21} & J_{11} \end{bmatrix} \begin{bmatrix} \frac{\partial u}{\partial \xi} \\ \frac{\partial u}{\partial \eta} \end{bmatrix} \tag{A17}$$

$$\epsilon = \frac{1}{|J|} \begin{bmatrix} J_{22} & -J_{12} & 0 & 0 \\ 0 & 0 & -J_{21} & J_{11} \\ -J_{21} & J_{11} & J_{22} & -J_{12} \end{bmatrix} \left[\frac{\partial u}{\partial \xi}, \frac{\partial u}{\partial \eta}, \frac{\partial v}{\partial \xi}, \frac{\partial v}{\partial \eta}\right]^T \tag{A18}$$

$$\epsilon = A\ G\ U = B\ U \tag{A19}$$

$$\left[\frac{\partial u}{\partial \xi}, \frac{\partial u}{\partial \eta}, \frac{\partial v}{\partial \xi}, \frac{\partial v}{\partial \eta}\right]^T = \begin{bmatrix} 25\eta - 5 & 0 & 5 - 25\eta & 0 & 25\eta & 0 & -25\eta & 0 \\ 25\xi - 5 & 0 & -25\xi & 0 & 25\xi & 0 & 5 - 25\xi & 0 \\ 0 & 25\eta - 5 & 0 & 5 - 25\eta & 0 & 25\eta & 0 & -25\eta \\ 0 & 25\xi - 5 & 0 & -25\xi & 0 & 25\xi & 0 & 5 - 25\xi \end{bmatrix} [u_1, u_2, u_3, u_4, u_5, u_6, u_7, u_8]^T \tag{A20}$$

$$\mathrm{B = AG} \tag{A21}$$

$$\frac{1}{2500}\begin{bmatrix} 50 & 0 & 0 & 0 \\ 0 & 0 & 0 & 50 \\ 0 & 50 & 50 & 0 \end{bmatrix} \begin{bmatrix} 25*0.042264-5 & 0 & 5-25*0.042264 & 0 & 25*0.042264 & 0 & -25*0.042264 & 0 \\ 25*0.157735-5 & 0 & -25*0.157735 & 0 & 25*0.157735 & 0 & 5-25*0.157735 & 0 \\ 0 & 25*0.042264-5 & 0 & 5-25*0.042264 & 0 & 25*0.042264 & 0 & -25*0.042264 \\ 0 & 25*0.157735-5 & 0 & -25*0.157735 & 0 & 25*0.157735 & 0 & 5-25*0.157735 \end{bmatrix} \tag{A22}$$

$$B = \frac{1}{2500}\begin{bmatrix} -197.17 & 0 & 197.17 & 0 & 52.83 & 0 & -52.83 & 0 \\ 0 & -52.83 & 0 & -197.17 & 0 & 197.17 & 0 & 52.83 \\ -52.83 & -197.17 & -197.17 & 197.17 & 197.17 & 52.83 & 52.83 & -52.83 \end{bmatrix} \tag{A23}$$

The stiffness matrix is given by $\int_v \; B^T DB\ dv = t \iint_0^{1/5} B^T DB \left|J_{\xi,\eta}\right| \left|J_{\bar{\xi},\bar{\eta}}\right| d\xi\ d\eta * weight$

The numerical integration is performed using 2 x 2 Gauss integration, where D is the constitutive matrix in plane stress condition.

$$\frac{E}{1-\nu^2}\begin{bmatrix} 1 & \nu & 0 \\ \nu & 1 & 0 \\ 0 & 0 & \frac{1-\nu}{2} \end{bmatrix} = \frac{2\ 10^5}{1-0.3^2}\begin{bmatrix} 1 & 0.3 & 0 \\ 0.3 & 1 & 0 \\ 0 & 0 & 0.35 \end{bmatrix} \tag{A24}$$

The value of B^TDB $\left|J_{\xi,\eta}\right| \left|J_{\bar{\xi},\bar{\eta}}\right|$ is as shown in the Table A1.

Table A1. The B^TDB $\left|J_{\xi,\eta}\right| \left|J_{\bar{\xi},\bar{\eta}}\right|$ matrix for element 1 at $(0.157735, 0.0422649)$

35035.523	5952.421	-30971.581	7047.798	-12362.484	-11111.740	8298.542	-1888.4791
5952.421	14415.599	9214.501	-2804.335	-12697.880	-12362.587	-2469.0424	751.323
-30971.581	9214.501	46138.408	-22214.721	-2804.342	7047.894	-12362.484	5952.325
7047.798	-2804.335	-22214.721	46138.126	9214.584	-30971.203	5952.339	-12362.587
-12362.48	-12697.880	-2804.342	9214.584	14415.331	5952.242	751.495	-2468.946
-11111.740	-12362.587	7047.894	-30971.203	5952.242	35035.049	-1888.396	8298.741
8298.542	-2469.0423	-12362.484	5952.339	751.495	-1888.396	3312.446	-1594.899
-1888.479	751.323	5952.325	-12362.587	-2468.946	8298.741	-1594.899	3312.522

A.1.1.2 Derive the Stiffness matrix at integration point (0.157735, 0.157735)

$$\frac{\partial x}{\partial \xi}=\frac{\partial}{\partial \xi}(N_1M_1X_1\ +\ N_2M_1X_2\ +\ N_2M_2X_3\ +\ N_1M_2X_4\,) \tag{A25}$$

$$\frac{\partial x}{\partial \xi}=(-5)(1-5*0.157735)(0)+\ (5)(1-5*0.157735)*10+(5)(5*0.157735)*10+\ (5)(-5*0.157735)*(0)=\ 50 \tag{A26}$$

$$\frac{\partial y}{\partial \xi}=\frac{\partial}{\partial \xi}(N_1M_1Y_1\ +\ N_2M_1Y_2\ +\ N_2M_2Y_3\ +\ N_1M_2Y_4\,) \tag{A27}$$

$$\frac{\partial y}{\partial \xi}=(-5)(1-5*0.157735)(0)+\ (5)(1-5*0.157735)*0+(5)(5*0.157735)*10+\ (5)(-5*0.157735)*(10)=\ 0 \tag{A28}$$

$$\frac{\partial x}{\partial \eta}=\frac{\partial}{\partial \eta}(N_1M_1X_1\ +\ N_2M_1X_2\ +\ N_2M_2X_3\ +\ N_1M_2X_4\,) \tag{A29}$$

$$\frac{\partial x}{\partial \eta}=(-5)(1-5*0.157735)(0)+(5*0.157735)(-5)(10)+(5)(5*0.157735)*10+(1-5*0.157735)(5)*0=0 \tag{A30}$$

$$\frac{\partial y}{\partial \eta}=\frac{\partial}{\partial \eta}(N_1M_1Y_1\ +\ N_2M_1Y_2\ +\ N_2M_2Y_3\ +\ N_1M_2Y_4\,) \tag{A31}$$

$$\frac{\partial y}{\partial \eta}=(-5)(1-5*0.157735)(0)+(5*0.157735)(-5)(0)+(5)(5*0.157735)*10+(1-5*0.157735)(5)*10=50 \tag{A32}$$

$$B=\frac{1}{2500}\begin{bmatrix} -52.83 & 0 & 52.83 & 0 & 197.168 & 0 & -197.168 & 0 \\ 0 & -52.83 & 0 & -197.168 & 0 & 197.168 & 0 & 52.83 \\ -52.83 & -52.83 & -197.168 & 52.83 & 197.168 & 197.168 & 52.83 & -197.168 \end{bmatrix} \tag{A33}$$

The value of $B^TDB\ |J_{\xi,\eta}|\ |J_{\bar{\xi},\bar{\eta}}|$ is as shown in the Table A2.

Table A2. The $B^TDB\ |J_{\xi,\eta}|\ |J_{\bar{\xi},\bar{\eta}}|$ matrix for element 1 at (0.157735, 0.157735)

3312.562	1594.937	751.379	1888.4413	-12362.643	-5952.383	8298.7007	2469.0046
1594.937	3312.5629	2469.0046	8298.7007	-5952.383	-12362.643	1888.4413	751.3794
751.379	2469.0046	14415.447	-5952.3837	-2804.183	-9214.443	-12362.643	12697.822
1888.441	8298.700	-5952.383	35035.090	-7047.753	-30971.147	11111.695	-12362.643
-12362.643	-5952.383	-2804.18388	-7047.7536	46137.975	22214.580	-30971.1480	-9214.443
-5952.3837	-12362.643	-9214.443	-30971.148	22214.580	46137.9750	-7047.753	-2804.183
8298.700	1888.441	-12362.643	11111.695	-30971.147	-7047.753	35035.090	-5952.383
2469.0046	751.3794	12697.822	-12362.643	-9214.443	-2804.1838	-5952.383	14415.447

A.1.1.3 Derive the Stiffness matrix at integration point (0.0422649, 0.0422649)

$$\frac{\partial x}{\partial \xi}=\frac{\partial}{\partial \xi}(N_1M_1X_1\ +\ N_2M_1X_2\ +\ N_2M_2X_3\ +\ N_1M_2X_4\,) \tag{A34}$$

$$\frac{\partial x}{\partial \xi}=(-5)(1-5*0.0422649)(0)+\ (5)(1-5*0.0422649)*10+(5)(5*0.0422649)*10+\ (5)(-5*0.0422649)*(0)=\ 50 \tag{A35}$$

$$\frac{\partial y}{\partial \xi}=\frac{\partial}{\partial \xi}(N_1M_1Y_1\ +\ N_2M_1Y_2\ +\ N_2M_2Y_3\ +\ N_1M_2Y_4\,) \tag{A36}$$

$$\frac{\partial y}{\partial \xi}=(-5)(1-5*0.0422649)(0)+\ (5)(1-5*0.0422649)*0+(5)(5*0.0422649)*10+\ (5)(-5*0.0422649)*(10)=\ 0 \tag{A37}$$

$$\frac{\partial x}{\partial \eta}=\frac{\partial}{\partial \eta}(N_1M_1X_1\ +\ N_2M_1X_2\ +\ N_2M_2X_3\ +\ N_1M_2X_4\,) \tag{A38}$$

$$\frac{\partial x}{\partial \eta}=(-5)(1-5*0.0422649)(0)+(5*0.0422649)(-5)(10)+(5)(5*0.0422649)*10+(1-5*0.0422649)(5)*0=0 \tag{A139}$$

$$\frac{\partial y}{\partial \eta}=\frac{\partial}{\partial \eta}(N_1M_1Y_1\ +\ N_2M_1Y_2\ +\ N_2M_2Y_3\ +\ N_1M_2Y_4\,) \tag{A40}$$

$$\frac{\partial y}{\partial \eta}=(-5)(1-5*0.0422649)(0)+(5*0.0422649)(-5)(0)+(5)(5*0.0422649)*10+(1-5*0.0422649)(5)*10=50 \tag{A41}$$

$$B=\frac{1}{2500}\begin{bmatrix} -197.168 & 0 & 197.168 & 0 & 52.83 & 0 & -52.83 & 0 \\ 0 & -197.16 & 0 & -52.83 & 0 & 52.83 & 0 & 197.168 \\ -197.168 & -197.168 & -52.83 & 197.168 & 52.83 & 52.83 & 197.168 & -52.83 \end{bmatrix} \tag{A42}$$

The value of $B^TDB\ |J_{\xi,\eta}|\ |J_{\bar{\xi},\bar{\eta}}|$ is as shown in the Table A3.

Table A3. The $B^TDB\ |J_{\xi,\eta}|\ |J_{\bar{\xi},\bar{\eta}}|$ matrix for element 1 at (0.0422649, 0.0422649)

46138.0334	22214.608	-30971.196	-9214.463	-12362.621	-5952.373	-2804.214	-7047.772
22214.608	22214.608	46138.033	-7047.772	-2804.214	-5952.373	-12362.621	-9214.463
-30971.196	-7047.772	35035.1296	-5952.373	8298.6890	1888.4407	-12362.621	11111.7049
-9214.462	-2804.214	-5952.373	14415.451	2469.00253	751.385	12697.833	-12362.621
-12362.621	-5952.373	8298.689	2469.0025	3312.5472	1594.930	751.385	1888.440
-5952.373	-5952.373	-12362.621	1888.4408	751.3854	1594.930	3312.547	2469.002
-2804.214	-2804.214	-9214.4629	-12362.621	12697.8339	751.3854	2469.0025	14415.451
-7047.772	-7047.772	-30971.1969	11111.7049	-12362.621	1888.4407	8298.6890	-5952.373

A.1.1.4 Derive the Stiffness matrix at integration point (0.0422649, 0.157735)

$$\frac{\partial x}{\partial \xi} = \frac{\partial}{\partial \xi}(N_1M_1X_1 + N_2M_1X_2 + N_2M_2X_3 + N_1M_2X_4) \tag{A43}$$

$$\frac{\partial x}{\partial \xi} = (-5)(1-5*0.157735)(0) + (5)(1-5*0.157735)*10 + (5)(5*0.157735)*10 + (5)(-5*0.157735)*(0) = 50 \tag{A44}$$

$$\frac{\partial y}{\partial \xi} = \frac{\partial}{\partial \xi}(N_1M_1Y_1 + N_2M_1Y_2 + N_2M_2Y_3 + N_1M_2Y_4) \tag{A45}$$

$$\frac{\partial y}{\partial \xi} = (-5)(1-5*0.0422649)(0) + (5)(1-5*0.0422649)*0 + (5)(5*0.0422649)*10 + (5)(-5*0.0422649)*(10) = 0 \tag{A46}$$

$$\frac{\partial x}{\partial \eta} = (-5)(1-5*0.157735)(0) + (5*0.157735)(-5)(10) + (5)(5*0.157735)*10 + (1-5*0.157735)(5)*0 = 0 \tag{A47}$$

$$\frac{\partial x}{\partial \eta} = \frac{\partial}{\partial \eta}(N_1M_1X_1 + N_2M_1X_2 + N_2M_2X_3 + N_1M_2X_4) \tag{A48}$$

$$\frac{\partial y}{\partial \eta} = \frac{\partial}{\partial \eta}(N_1M_1Y_1 + N_2M_1Y_2 + N_2M_2Y_3 + N_1M_2Y_4) \tag{A49}$$

$$\frac{\partial y}{\partial \eta} = (-5)(1-5*0.0422649)(0) + (5*0.0422649)(-5)(0) + (5)(5*0.0422649)*10 + (1-5*0.0422649)(5)*10 = 50 \tag{A50}$$

$$B = \frac{1}{2500}\begin{bmatrix} -52.83 & 0 & 52.83 & 0 & 197.168 & 0 & -197.168 & 0 \\ 0 & -197.16 & 0 & -52.83 & 0 & 52.83 & 0 & 197.168 \\ -197.168 & -52.83 & -52.83 & 52.83 & 52.83 & 197.168 & 197.168 & -52.83 \end{bmatrix} \tag{A51}$$

The value of $B^TDB\ |J_{\xi,\eta}|\ |J_{\bar{\xi},\bar{\eta}}|$ is as shown in the Table A4.

Table A4. The $B^TDB\ |J_{\xi,\eta}|\ |J_{\bar{\xi},\bar{\eta}}|$ matrix for element 1 at (0.0422649, 0.157735)

14415.462	5952.387	751.373	-2469.008	-12362.637	-12697.828	-2804.198	9214.448
5952.387	5952.387	35035.133	-1888.445	8298.684	-11111.700	-12362.627	7047.758
751.373	751.373	-1888.445	3312.558	-1594.933	8298.704	-2468.998	-12362.637
-2469.008	-2469.008	8298.684	-1594.933	3312.551	-1888.437	751.391	5952.379
-12362.637	-11111.700	8298.7048	-1888.436	35035.086	5952.369	-30971.153	7047.767
-12697.828	-12362.627	-2468.998	751.391	5952.369	14415.436	9214.457	-2804.199
-2804.198	-2804.198	7047.758	-12362.637	5952.379	-30971.153	9214.457	46137.990
9214.449	9214.449	-30971.191	5952.377	-12362.62	7047.767	-2804.199	-22214.594

Stiffness Matrix for element 1

The stiffness matrix for the element 1 is as shown in the Table A5.

A.1.1.5 Applying Boundary Conditions

The nodal displacements at nodes 1, 4, 6, 8, 10, 12 having supports are equal to zero. The degrees of freedom are $U_1 = U_2 = U_7 = U_8 = U_{11} = U_{12} = U_{15} = U_{16} = U_{19} = U_{20} = U_{23} = U_{24} = 0$ and for force vector we have $F_{61} = -1257$ N, $F_{63} = F_{65} = F_{67} = F_{69} = -2514$ N, $F_{71} = -1257$ N.

Table A5. The stiffness matrix for element 1

98901.582	35714.355	-60440.0250	-2747.231	-49450.387	-35714.325	10988.829	2747.202
35714.355	98901.329	2747.2889	10988.8354	-35714.338	-49450.479	-2747.305	-60439.684
-60440.0249	2747.288	98901.544	-35714.4125	10988.867	-2747.10688	-49450.387	35714.230
-2747.231	10988.835	-35714.412	98901.219	2747.3960	-60439.575	35714.248	-49450.479
-49450.387	-35714.338	10988.867	2747.3960	98900.9401	35714.123	-60439.420	-2747.1809
-35714.326	-49450.479	-2747.1067	-60439.575	35714.1235	98901.0081	2747.3095	10989.0468
10988.829	-2747.3058	-49450.387	35714.248	-60439.420	2747.3094	98900.978	-35714.251
2747.2023	-60439.685	35714.230	-49450.4798	-2747.180	10989.0468	-35714.252	98901.1179

A.1.2 Calculate the nodal displacements

The steps followed to determine the nodal displacements at each node are as follows:

1. Forming the global stiffness matrix (K) and global force vector (F)
2. Applying the boundary condition
3. Eliminating the rows and columns having zero displacements
4. The nodal displacements (U) can be solved using the relation KU = F

The plate structure is modelled using MARC Mentat as shown in Fig.A.1. The static analysis is performed and the nodal displacements along X and Y directions are gotten as shown in Fig.A.2 and Fig.A.3, respectively. The acquired nodal displacements using IGA and MARC Mentat® are similar and tabulated as shown in Table A6. The results show that the acquired nodal displacements using IGA are in good agreement with the nodal displacements achieved via a commercial package MARC Mentat ®.

Table A6. The nodal displacements along X and Y directions

Node	X-Displ	Y-Displ	Node	X-Displ	Y-Displ
1	0	0	19	-0.0374185	-0.00943319
2	-0.0136164	-0.00679161	20	-0.0368242	-0.00571293
3	-0.0115093	-0.0032123	21	-0.0363293	-0.00191491
4	0	0	22	-0.0363293	0.00191491
5	-0.0112979	-0.000975359	23	-0.0368242	0.00571293
6	0	0	24	-0.0374185	0.00943319
7	-0.0112979	0.000975359	25	-0.049715	-0.00962066
8	0	0	26	-0.0493922	-0.00583879
9	-0.0115093	0.0032123	27	-0.0490678	-0.00195904
10	0	0	28	-0.0490678	0.00195904
11	-0.0136164	0.00679161	29	-0.0493922	0.00583879
12	0	0	30	-0.049715	0.00962066
13	-0.0254742	-0.00873329	31	-0.0622312	-0.00980279
14	-0.0242224	-0.00517617	32	-0.0619778	-0.0059837
15	-0.0235815	-0.00164667	33	-0.0617344	-0.0020241
16	-0.0235815	0.00164667	34	-0.0617344	0.0020241
17	-0.0242224	0.00517617	35	-0.0619778	0.0059837
18	-0.0254742	0.00873329	36	-0.0622312	0.00980279

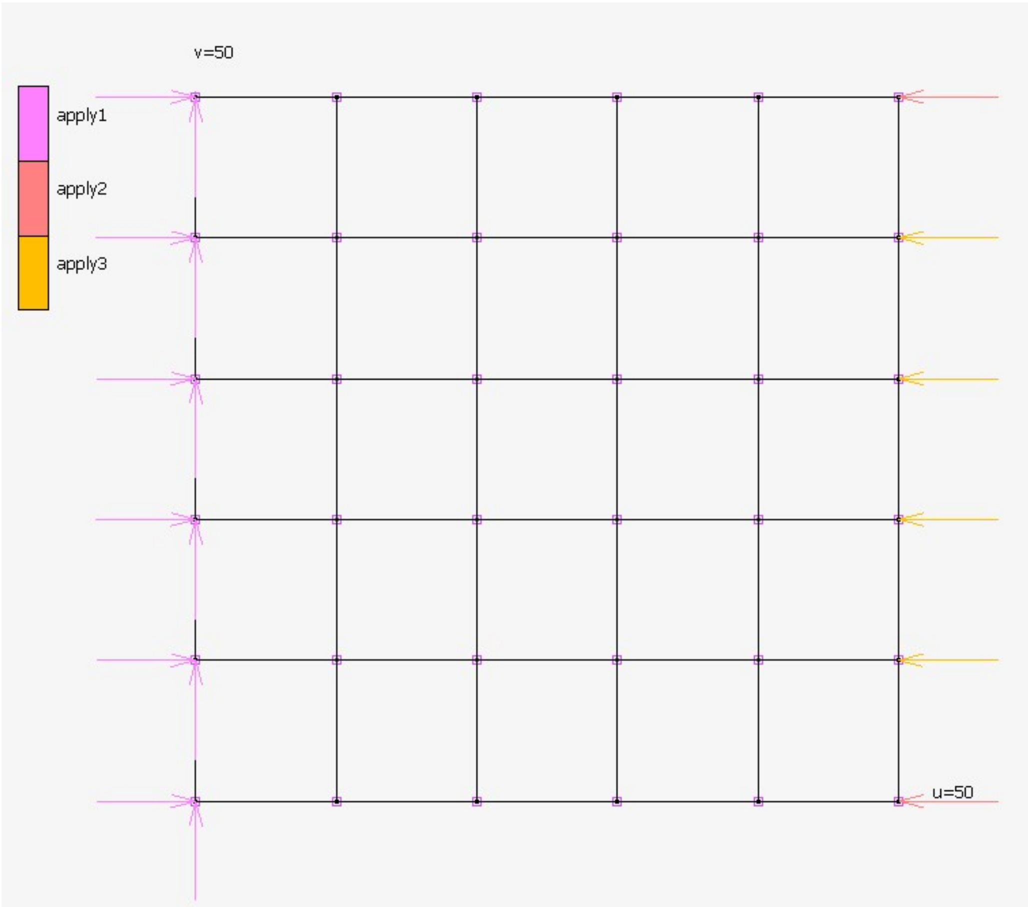

Fig. A.1. The loading case in Marc Mentat®

Fig. A.2. The nodal X-displacement performing FEA using MSc Marc®

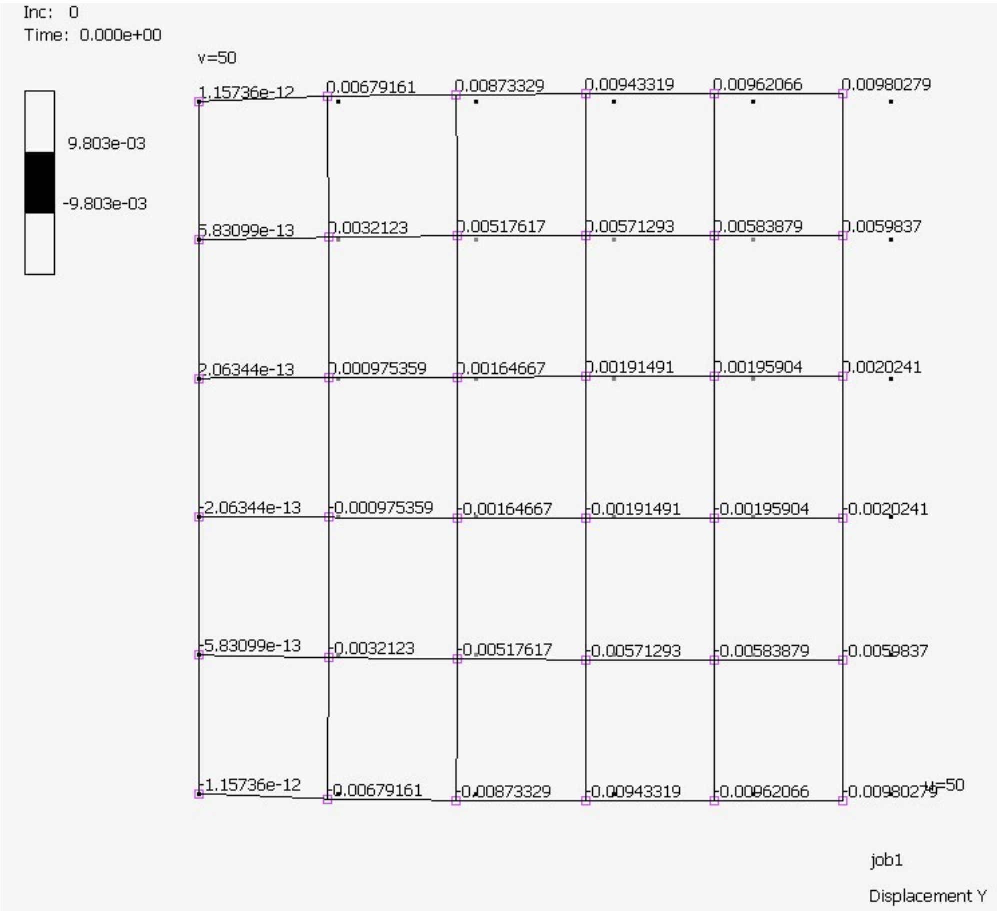

Fig. A.3. The nodal Y-displacement performing FEA using MSc Marc ®